Glassy behaviour in a 3-state spin model

2001 J. Phys. A: Math. Gen. 34 5147

(http://iopscience.iop.org/0305-4470/34/25/302)

INSTITUTE OF PHYSICS PUBLISHING JOURNAL OF PHYSICS A: MATHEMATICAL AND GENERAL

J. Phys. A: Math. Gen. **34** (2001) 5147–5182 PII: S0305-4470(01)21007-5

Glassy behaviour in a 3-state spin model

Lexie Davison, David Sherrington, Juan P Garrahan and Arnaud Buhot

Theoretical Physics, University of Oxford, 1 Keble Road, Oxford OX1 3NP, UK

E-mail: ldavison@thphys.ox.ac.uk, d.sherrington1@physics.ox.ac.uk, j.garrahan1@physics.ox.ac.uk and buhot@thphys.ox.ac.uk

Received 15 January 2001, in final form 17 April 2001
Published 15 June 2001
Online at stacks.iop.org/JPhysA/34/5147

Abstract

In this paper we study a simple spin model which has a non-interacting Hamiltonian but constrained dynamics. The model, which is a simplification of a purely topological cellular model (Davison L and Sherrington D 2000 *J. Phys. A: Math. Gen.* **33** 8615, Aste T and Sherrington D 1999 *J. Phys. A: Math. Gen.* **32** 7049), displays glassy behaviour, involves activated processes and exhibits two-step relaxation. This is a consequence of the existence of annihilation–diffusion processes on two distinct timescales, one temperature independent and the other an exponential function of inverse temperature. In fact, there are several such inter-coupled microscopic processes and great richness therein. Two versions of the model are considered, one with a single absorbing ground state and the other with a highly degenerate ground state. These display qualitatively similar but quantitatively distinct macroscopic behaviour and related, but different, microscopic behaviour.

PACS numbers: 7510, 0550, 0240

1. Introduction

In a recent paper Davison and Sherrington [1] focussed on a purely topological tiling model [2] which exhibited glassy dynamical behaviour. This was driven by a desire to investigate the behaviour of supercooled liquids in a model which contained as few parameters as possible, but still displayed the relevant physics. In this paper we continue the minimalistic approach, and consider systems which are conceptually similar to the topological model, but have the major advantage of involving variables (spins) based on a fixed lattice.

The original model was that of a two-dimensional topological froth, constructed by tiling the plane using three-fold vertices only. However, unlike soap froths, the energy was determined by the deviation of the cell topologies from a perfect hexagonal tiling: $E = \sum_i^N (n_i - 6)^2$, where n_i is the number of sides of cell i, and the system evolved solely

through stochastic T1-micro-dynamics with Glauber–Kawasaki probabilities. We found that there was two-step relaxation at low temperatures, and formed the following conceptual picture describing the evolution of the system. At low temperatures the system consists mainly of six-sided cells, and there are two processes dominating the behaviour: on a fast timescale, pairs of pentagon–heptagon defects diffuse freely through the hexagonal background, and on a slower timescale isolated defects absorb or create pairs of defects. The latter can be considered to be an activated process, as it is energetically unfavourable for such a pair of defects to be created. This conceptual framework of two different processes leading to both fast and slow dynamics is directly applicable to the lattice-based spin model with which this paper is concerned, and thus one might expect it to yield qualitatively similar results to the topological model. Given that this spin model is computationally simpler and more tractable, one might hope to be able to probe more deeply, and to investigate to what extent one finds the same features displayed by other kinetically constrained models (for examples see [3–11]). In fact, as we show below, these expectations are borne out and it is possible to provide a physical understanding of the features observed. It is also both possible and instructive to consider a generalization with a very different (highly degenerate) ground state, which we cover in the latter half of the paper.

2. The model

The model we use comprises a perfect hexagonal tiling of the plane, with a variable (spin) associated with each hexagon. The spin in cell i, denoted by s_i, is restricted to the values $0, \pm 1$. This is analogous to a topological froth in which the cells are all pentagons, hexagons or heptagons, so that the topological charge $q_i = (6 - n_i)$ of each cell is restricted to the values $0, \pm 1$. However, the topological froth model has a non-periodic and dynamically changing cell structure, whereas this model is firmly fixed on a perfect hexagonal tiling.

We define the energy as follows:

$$E = D \sum_{i=1}^{N} s_i^2 \tag{1}$$

where N is the total number of cells/spins in the system, and D may be positive or negative. The case of $D > 0$ emulates the original topological model where hexagonal order is energetically preferable, but $D < 0$ is also of interest, as we shall show. The dynamics conserve the total spin of the system and we choose our starting configuration such that the total spin is always zero, i.e.

$$\sum_{i=1}^{N} s_i = 0 \tag{2}$$

in analogy with the Euler rule $\sum_i^N (6 - n_i) = 0$ which applies to a froth [12, 13]. Therefore the ground state for $D > 0$ consists of $s_i = 0$ for all spins, whereas for $D < 0$ the ground state is degenerate, with half the spins taking the value +1 and half taking the value -1.

The system is allowed to evolve through local spin-flips which are similar to the T1 moves performed on topological froths. In the latter two adjacent cells have their topological charges decreased by 1, and their two common neighbours have their topological charges increased by 1: see figure 1(*a*). In the present model the allowed move-sets consist of choosing a pair of neighbouring cells and either increasing their spins by 1 unit, and decreasing those of their common neighbours by 1 unit, or vice versa; both possibilities need to be allowed to avoid chirality inhibiting movement of spins throughout the system.

The actual dynamical process is as follows. At each time step an edge is chosen randomly on the hexagonal lattice; this defines a set of four cells as shown in figure 1(*b*). A choice is then

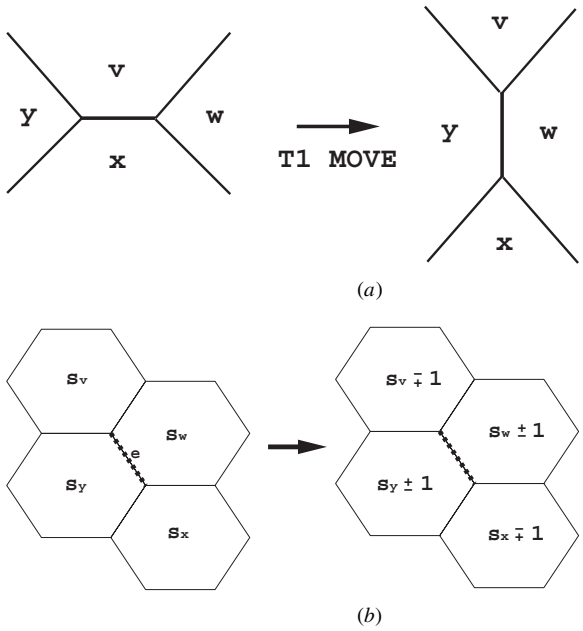

Figure 1. Spin-flip rules for the 3-state spin model and the topological froth. (*a*) The T1 moves for the topological froth. (*b*) The spin-flip rules for the present model: the total spin is conserved and the choice of whether to attempt the upper or lower signs is made randomly at each time-step. The quadruplet of cells is identified uniquely by the dashed edge e.

made randomly of whether to consider increasing the spins of the adjacent cells y and w (and thus decreasing v, x) or vice versa, with equal probabilities for both cases. The probability of actually performing the move is dependent on the energy change that would be incurred, and is given by a temperature-dependent Metropolis–Kawasaki[1] algorithm. Specifically, assuming w and y have been chosen as candidates for an increase in spin, the energy change associated with these spin-flips on spins s_v, s_w, s_x, s_y is:

$$\Delta E(s_w, s_y; s_v, s_x) = 2D(2 + s_w + s_y - s_v - s_x) \tag{3}$$

and the probability P of actually performing this move is:

$$P(s_w, s_y; s_v, s_x) = (1 - \delta_{s_w,1})(1 - \delta_{s_y,1})(1 - \delta_{s_v,-1}) \times (1 - \delta_{s_x,-1})\mathrm{Min}[1, \exp(-\beta \Delta E(s_w, s_y; s_v, s_x))] \tag{4}$$

where β is the inverse temperature. The δ-functions ensure that the spins are forbidden to take values other than ± 1 or 0.

The simple form of equation (1), with no interaction between the cells, shows that this system is thermodynamically trivial in equilibrium and all the static equilibrium properties are readily calculable. However, the microscopic dynamics are constrained and non-trivial, involving several spins simultaneously; this leads to glassy macro-dynamics.

Most of the data results from simulations on a system of size $N = 9900$, although, in order to perform more accurate fits, in certain cases the system size was increased to 160 000.

[1] We choose to use the Metropolis algorithm rather than Glauber dynamics as in previous work because the qualitative features of the results show no dependence on which of these algorithms we choose, and Metropolis is the faster of these two. The reference to Kawasaki is included to emphasize the fact that although more than one spin is flipped at once, the total spin is conserved.

However, unless otherwise stated, one should assume the former system size is in use. Periodic boundary conditions are enforced in all cases.

This paper is structured in the following manner: first we present results for $D > 0$, including a discussion on the processes involved in relaxation of the system; this is followed with results for $D < 0$. Finally there is a more general discussion.

2.1. Brief review of the topological froth model

As one of the aims of this paper is to show that the behaviour of this model is indeed qualitatively very similar to that of the topological froth, we shall briefly review the results for the topological froth before proceeding [1, 2].

In simulations in which the system is cooled at a variety of different rates, one finds strong dependence of the energy on the cooling rate, with the system unable to attain equilibrium within any reasonable timescale at very low temperatures. Measurements of a two-time auto-correlation function show evidence of two-step relaxation, with plateaux developing as the temperature is reduced. There are also clear signs of aging when the system is not in equilibrium. When the equilibrium correlation functions are rescaled by a suitably defined relaxation time, one finds that they collapse onto a master curve in the late-β relaxation regime, and that this master curve can be fitted by a von Schweidler law as predicted by mode-coupling theory (MCT) [14]. The relaxation time is well described by an offset Arrhenius law, indicating strong glassy behaviour [15]. Although MCT in fact predicts a power law, this does not fit the data particularly well, and neither does the often-used Vogel–Fulcher law.

By measuring a suitable temporal response function and plotting it parametrically against the appropriate correlation function (starting from a non-equilibrium configuration), the fluctuation–dissipation theorem (FDT) is found to be upheld for times somewhat longer than required for the onset of the correlation function plateaux. For longer times FDT ceases to hold. After it is broken, one observes non-monotonic behaviour, a feature which has also been noted in several other models which can be considered to involve activation over energy barriers [3–9, 16].

3. $D > 0$

3.1. Relaxation dynamics

It is a simple matter to calculate the equilibrium behaviour of $\frac{E}{N}$, for which one finds (in units of $D = 1$)

$$\frac{E}{N} = \frac{2\exp(-\beta)}{1 + 2\exp(-\beta)}. \tag{5}$$

One has instant access to equilibrium states, as one can randomly place the appropriate number of ± 1's throughout the system to access a particular temperature. Using this feature, we may study the behaviour of the energy with temperature at a number of different cooling rates, starting from equilibrium at any chosen temperature. Above $T = 1$ the system equilibrates very rapidly at even the fastest cooling rate, so we have chosen a starting configuration of $T = 1$, and then cooling is carried out by waiting a time $t_w = \gamma N$ at each temperature decrement of $\delta T = 0.05$. The results (averaged over three runs), with the equilibrium curve, are shown in figure 2(*a*); the system exhibits strong dependence of the energy upon the cooling rate. This is characteristic of glassy systems, and qualitatively similar to the results found for the purely topological froth.

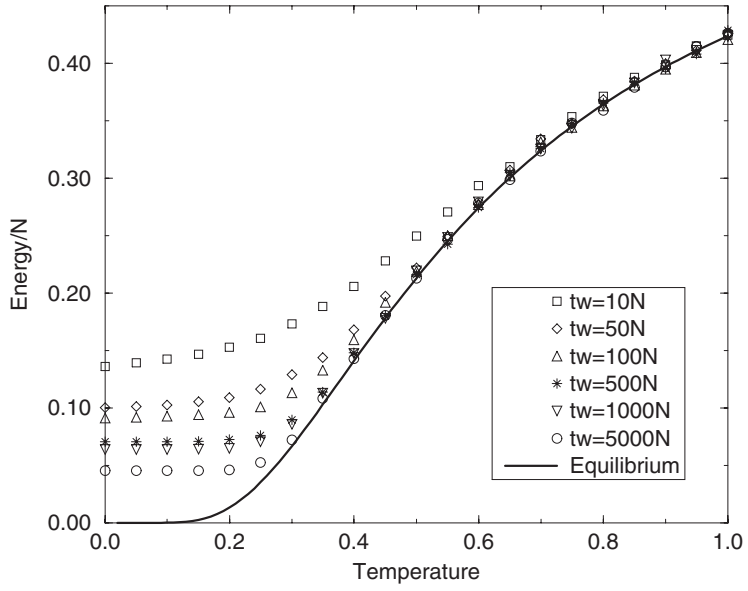

(*a*)

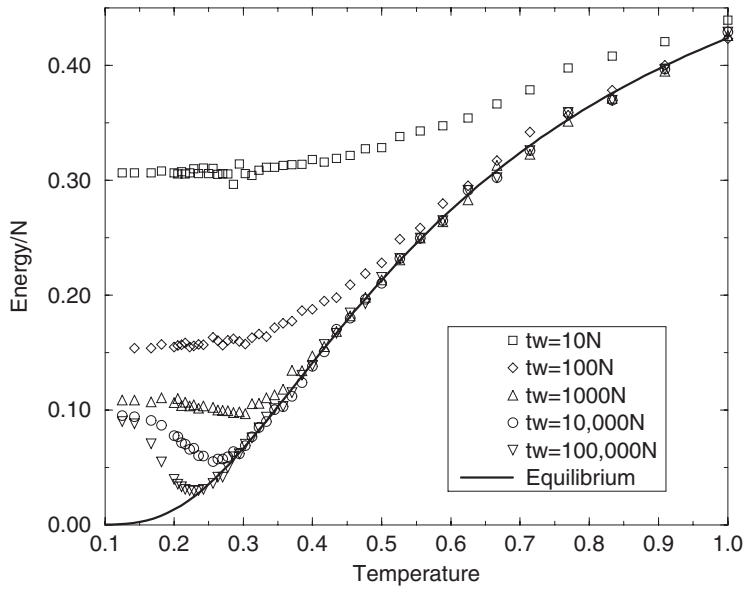

(*b*)

Figure 2. Energy against temperature for slow cooling and rapid quench. (*a*) The behaviour of the energy with temperature under slow cooling ($D > 0$). The values of t_w are the waiting times at each point. (*b*) The behaviour of the energy with temperature after a rapid quench ($D > 0$). The values of t_w are the times, subsequent to the quench, at which the energy is measured.

It is instructive to study also the behaviour of the system when subjected to a rapid quench from an infinite temperature ($\beta = 0$) configuration to a temperature at which it is allowed to evolve for a time t_w. Figure 2(*b*) shows the results from such a quench for a range of different temperatures. For longer values of t_w we see a minimum develop—this strongly suggests

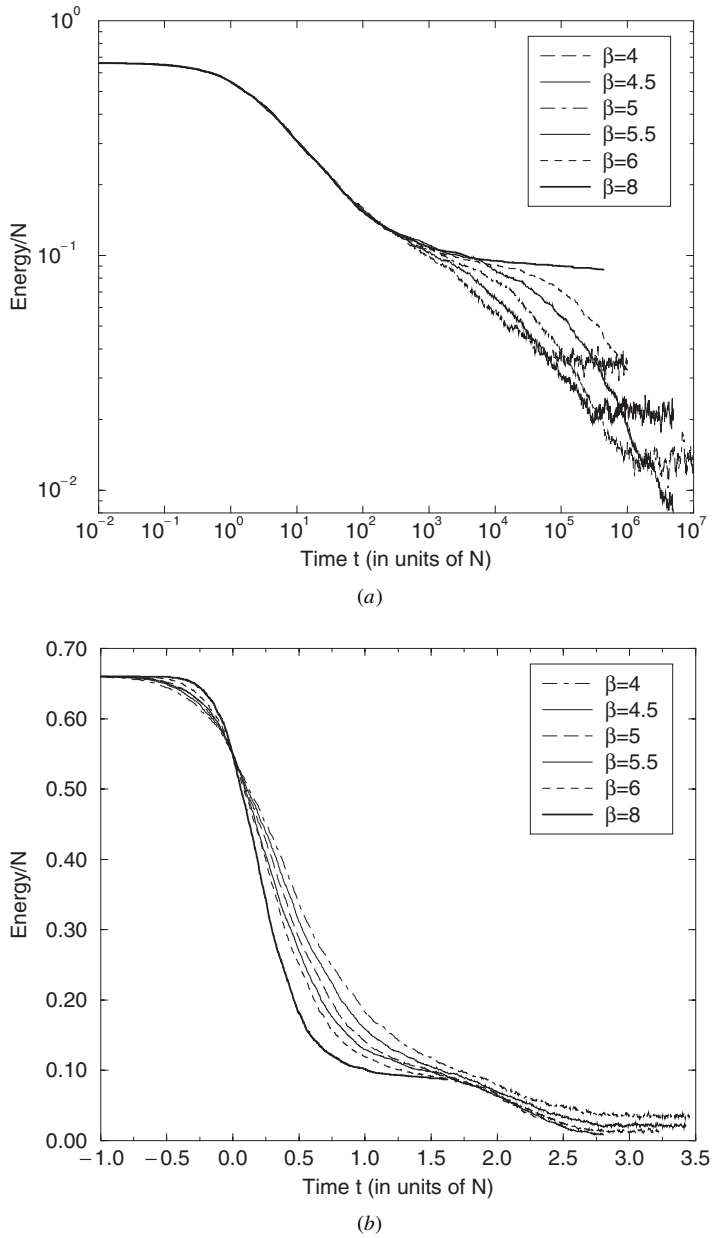

Figure 3. The behaviour of the energy with time. (*a*) Energy against time. The curves for $\beta \leqslant 5$ reach their equilibrium values, whereas the others do not. (*b*) Energy against $T \ln t$ (where t is measured in units of N).

activation is present: at very low temperatures the system cannot overcome the energy barriers and thus cannot access lower energy states. The temperature at which this minimum occurs is dependent on the waiting time t_w. At very low temperatures, even at the largest waiting times employed ($t_w = 100\,000N$) the system is unable to reach energies below $\frac{E}{N} \sim 0.09$.

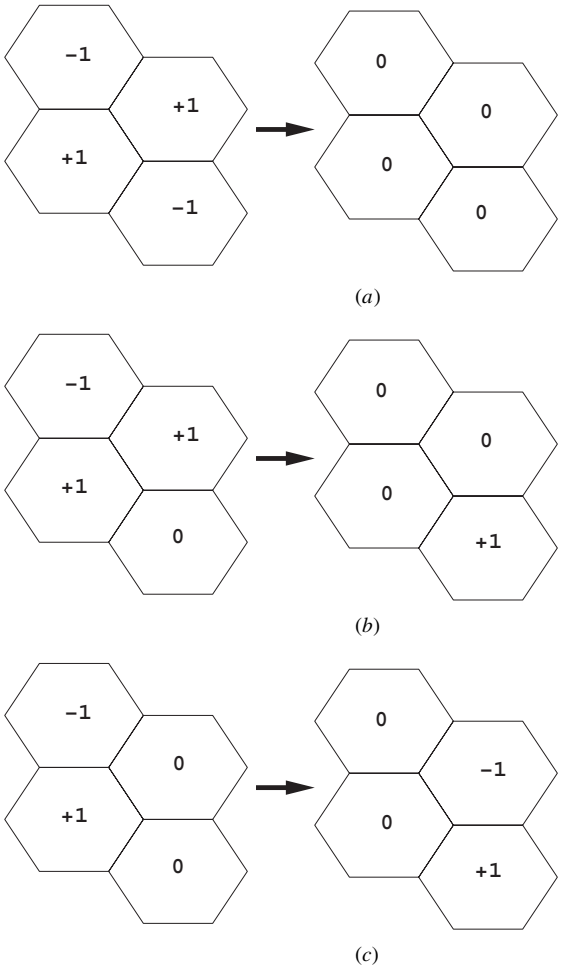

Figure 4. The dominant moves through which this model evolves. (*a*) Annihilation of two dimers. This is also possible if each spin is multiplied by -1. (*b*) Annihilation of a dimer through interaction with a defect. The defect is shifted in position. (*c*) Free diffusion of a dimer in a background of zero spins.

One sees the significance of this value if we turn to the temporal behaviour of the energy. Figure 3(*a*) is a plot of $\frac{E}{N}$ against time, quenched from a fully disordered starting configuration corresponding to $\beta = 0$ to the temperature in question. The initial decay of the energy is fast and independent of temperature until $\frac{E}{N} \sim 0.09$, at which point one sees the existence of a plateau; the time spent on this plateau is clearly dependent on temperature. Upon departure from the plateau, the energy relaxes directly to the appropriate equilibrium value; on the graph shown, the curves for $\beta \leqslant 5$ equilibrate within the timescale of the simulation, whereas those for $\beta > 5$ do not. This two-time behaviour, with one timescale temperature independent and the other increasing with inverse temperature, can be understood as follows. The mechanism for lowering the energy is the annihilation of pairs of adjacent +1 and -1 spins (we shall refer to a +1, -1 pair as a 'dimer'). This occurs in two ways: (i) two neighbouring conjugate dimers can destroy each other to leave four zero spins as shown in figure 4(*a*), with a reduction in energy of 4 units, or (ii) a ± 1 can annihilate a dimer, thus shifting its position and reducing the energy

by 2 units as in figure 4(b); note that the ± 1 can be part of a dimer at a different orientation. Any such local arrangements present in the starting configuration will be eliminated quickly without need of any thermal excitation. Furthermore, dimers can move freely through a background of zero spins as shown in figure 4(c) until they reach a local environment which favours annihilation, such as those previously mentioned. This diffusion occurs on a timescale of two steps per spin, as one can alter the configuration on the left of the arrow in figure 4(c) in two ways, one of which will be possible and one of which will be forbidden through the δ-functions in equation (4). Consequently, the initial fast decay of the energy is temperature independent, and of a diffusive character with an underlying timescale of 2. This fast, diffusive process describes the behaviour of the energy until the plateau is reached. To describe it further, one has to consider isolated defects, i.e. isolated spins of ± 1. To remove these defects, they must be paired up with a conjugate isolated defect to form a dimer which can then diffuse freely as in figure 4(c), and eventually annihilate as in figures 4(a) and (b). An isolated defect can move through fortuitous collisions with existing dimers, but after the initial fast decay these dimers become rare. Alternatively, a defect can move by creating a new dimer (reversing the arrow in figure 4(b)), at an activation energy cost of 2 units and with a probability that scales as $\mathrm{e}^{-2\beta}$. As is clear from this figure, one can interpret the resulting configuration as a dimer-plus-defect in two ways; either of these two possible dimers can diffuse away freely if adjacent to two zero spins, or annihilate if adjacent to another dimer. This factor of 2 will cancel that introduced by the diffusive timescale of the dimers. Thus again one has a diffusive process leading to a final reduction in energy, in this case with a timescale of $\mathrm{e}^{2\beta}$ (since the timescale for annihilation of the dimer is negligible compared to that to produce the dimer for $\mathrm{e}^{2\beta} \gg 1$). Thus $E(t)/N$ is expected to consist of two diffusive processes: a fast process of timescale 2 decaying to a state of isolated defects, and a slow process of timescale $\mathrm{e}^{2\beta}$ decaying to the equilibrium configuration.

The plateau in $E(t)/N$ can be seen more clearly if the time axis is rescaled to $T \ln t$ as in figure 3(b); as the temperature is decreased (β increased) the curves tend to a sharp staircase form. This is reminiscent of the results found under such rescaling for other kinetically constrained models [3–9]; in these other models one observes several plateaux corresponding to several characteristic activation energies, but in this particular case the situation is simpler as there is only one dominant characteristic activation energy.

Both the fast dimer–dimer annihilation and the slow defect–antidefect pairing are of the type usually designated as $A + B \rightarrow \emptyset$ [17–19]. In the fast process, A and B are dimers and 'anti-dimers', i.e. a $(+1, -1)$ dimer annihilating with a $(-1, +1)$ anti-dimer; for the slow process, A and B are isolated defects of opposite sign. In detail these diffusion processes are more complicated than simple diffusion, but for $A + B \rightarrow \emptyset$ processes the standard asymptotic behaviour of the density is of the form $t^{-\frac{d}{4}}$, where d is the dimensionality. Therefore we suggest the same asymptotic $(t/\tau)^{-0.5}$ behaviour for each process[2], and fit the following form to the energy:

$$\frac{E(t)}{N} = \left(\frac{2}{3} - a\right)\left(1 + \frac{t}{2}\right)^{-b} + (a - e_{\mathrm{eq}})\left(1 + \frac{t}{\mathrm{e}^{2\beta}}\right)^{-c} + e_{\mathrm{eq}} \tag{6}$$

where a is the plateau value, e_{eq} is the energy per spin in equilibrium, and we expect both b and c to be approximately 0.5. The results are shown in figure 5; it is clear that these fits are extremely good. In principle, the plateau value a can be calculated but here we note only that, as required, a is less than 0.25, which is the maximum energy for a $T = 0$ frozen state. It is also less than the value corresponding to randomly removing dimers from the initial configuration

[2] In fact, whilst the slow processes are isotropic, this is not the case for the fast dimer diffusion: the latter involves zig-zags at 30° to the axis perpendicular to the common edge between the two cells constituting the dimer.

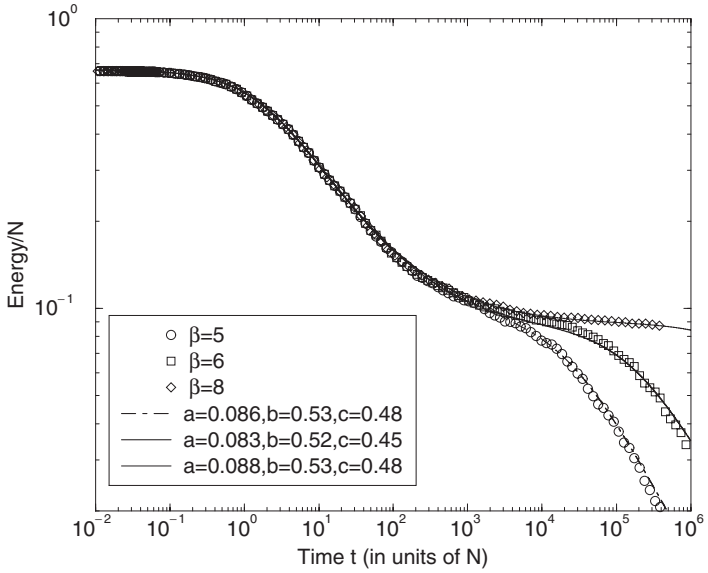

Figure 5. The energy fitted with equation (6), using the values shown in the key.

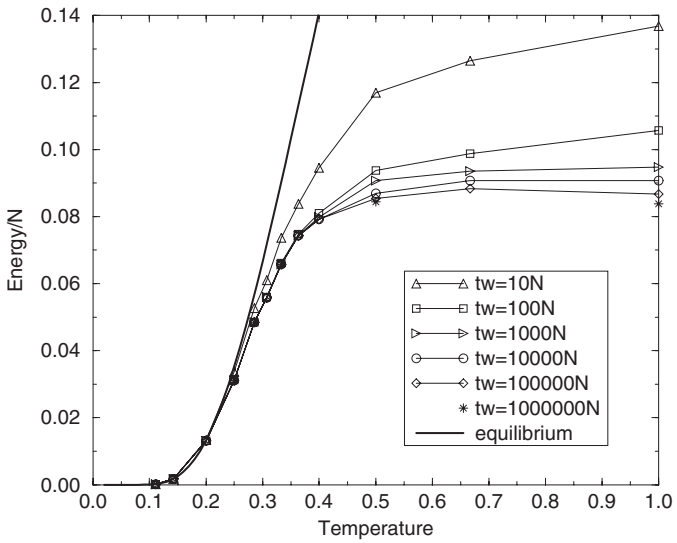

Figure 6. The behaviour of E/N after a $T = 0$ quench from equilibrium.

to leave only isolated defects, which gives $E(t)/N \simeq 0.2$; in fact, one finds $a \sim 0.085$ due to the effect of singleton pairing by dimer collisions. Further investigation of the characteristic timescales is given below, in connection with the correlation function.

The reader will note that the fast dimer absorption by an isolated defect has been neglected in the above fit; this can be characterised as type $A + C \rightarrow \emptyset + C$, and standard asymptotic behaviour of the density for such a process is that of a stretched exponential [18–21]. There is also a move-set which involves two dimers interacting 'off-centre', such that one of the dimers and only one of the defects in the other dimer are altered. This leaves either two isolated

defects or a dimer. However, in view of the excellent quality of the fit we do not consider these explicitly at this stage.

We have also investigated the behaviour of the energy if one quenches to $T = 0$ from an initial equilibrium configuration corresponding to a finite temperature T_I. This is in some sense an investigation of the inherent states of the system [22–26]. At very low temperatures, the equilibrium state for T_I consists mainly of isolated defects—thus when quenched to $T = 0$ the system very quickly reaches the inherent state. However, at higher initial temperatures this takes an extremely long time to happen. Thus we show in figure 6 the energy measured at waiting time t_w after a quench from the equilibrium configuration to $T = 0$. At low T_I the energy stays on the equilibrium curve, as there are no energetically favourable moves to be made. However, for higher T_I the energy tends towards a constant value given by the plateau in figure 6. Thus we see that if one quenches from an equilibrium configuration with energy above the plateau, the lowest energy one can reach is that of the plateau—to decrease energy further would require activated processes, which one cannot perform at $T = 0$. If one quenches from an equilibrium start-point with energy below that of the plateau, one cannot decrease the energy by much as there are very few energetically favourable moves to be made, and so the curves in figure 3 do not deviate far from the equilibrium curve. The temperature at which one sees a crossover between these two types of behaviour is $T \sim 0.35$: this is the temperature at which activated processes become important.

3.2. Correlation functions and relaxation time

We investigate the temporal correlations in the system through a two-time single-site spin correlation function of the form

$$C(t_w, t_w + t) = \frac{\sum_{i=1}^{N} s_i(t_w)s_i(t_w + t)}{\sum_{i=1}^{N} s_i^2(t_w)}. \tag{7}$$

Under equilibrium conditions this becomes a function of the relative time t only. The equilibrium correlation functions (averaged over five runs) for a range of temperatures are shown in figure 7(*a*). As β increases, plateaux develop, revealing that again two-step relaxation is taking place. We also show examples of typical out-of-equilibrium correlation functions in figure 7(*b*); one can see ageing behaviour, with the correlation function showing dependence on the waiting time t_w after a rapid quench from infinite temperature.

Following the procedure in [1,27], we may define a relaxation time τ_r as the time at which the equilibrium correlation function decays to e^{-1}. This is plotted in figure 8 against inverse temperature; the data can be reasonably fitted by an Arrhenius curve of the form

$$\tau_r = A e^{B/T} \tag{8}$$

where A, B are constants. The solid line superimposed on figure 8 corresponds to $A = 0.0166, B = 2.535$. This indicates that this model displays strong glassy behaviour, in agreement with the results from the topological model, where an offset Arrhenius law fitted the data considerably better than either a power law, or a Vogel–Fulcher law [1]. The anomalous upturn in the curve at very low β is due to the restriction that the spins may only take the values ± 1 or 0; when the density of non-zero spins is very high, it becomes likely that some defects will sit next to each other, in locally 'stuck' configurations which slow the decay of the correlation function (see figure 9).

However, if we look closely at figure 8, we see that at high inverse temperature the data seems to be drifting below the curve. If we consider more carefully the expected form of $C(t)$ it becomes clear that the above definition of τ_r is not the most appropriate one, since again, as in the topological model, there are two decay processes. One can understand the

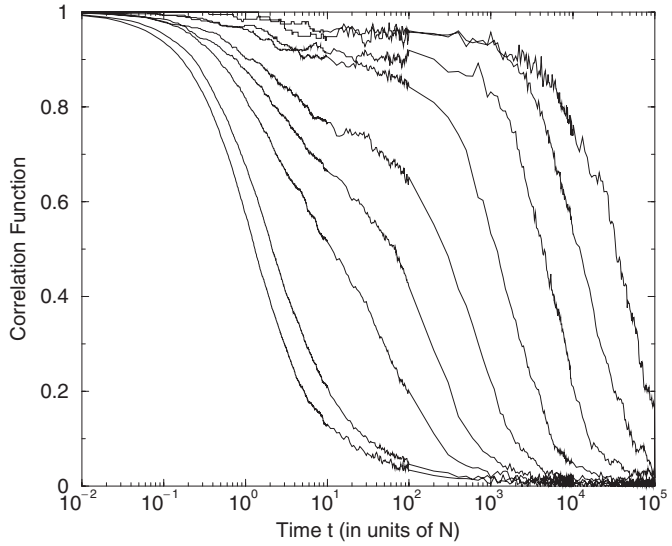

(*a*)

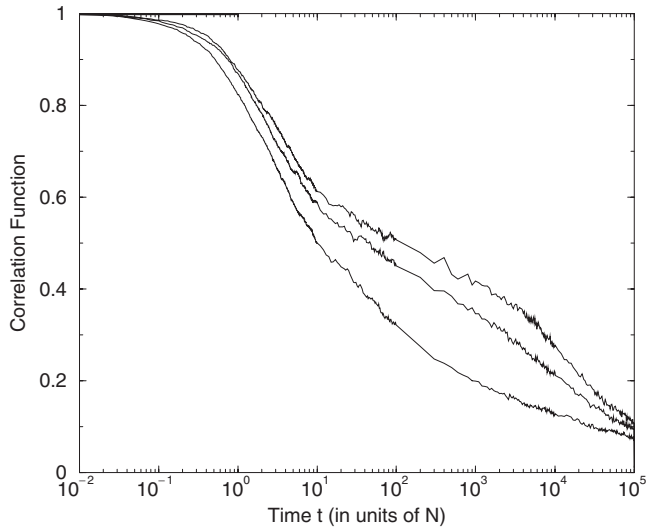

(*b*)

Figure 7. Correlation functions both in and out of equilibrium. (*a*) Equilibrium correlation functions $C(t)$ for (from left to right) $\beta = 1, 2, 3, 3.5, 4, 4.5, 5, 5.5, 6$. (*b*) Out of equilibrium correlation functions $C(t_w, t_w + t)$ for $\beta = 6$ for (from left to right) $t_w = 10^2 N, 10^3 N, 10^4 N$.

origin of the plateaux by considering further the dominant processes involved in evolution of the system, which are analogous to those in the topological model [1]. In equilibrium, at low temperatures (high β) there are few defects present in the system. The initial fast decay from $C(t = 0) = 1$ is due to dimers diffusing freely through the system, and thus moving the system away from the starting configuration. Isolated defects, however, need to either absorb or create a dimer in order to change position; this happens on a much longer timescale than diffusion of the dimers. Therefore again we have two timescales in the model—fast dynamics

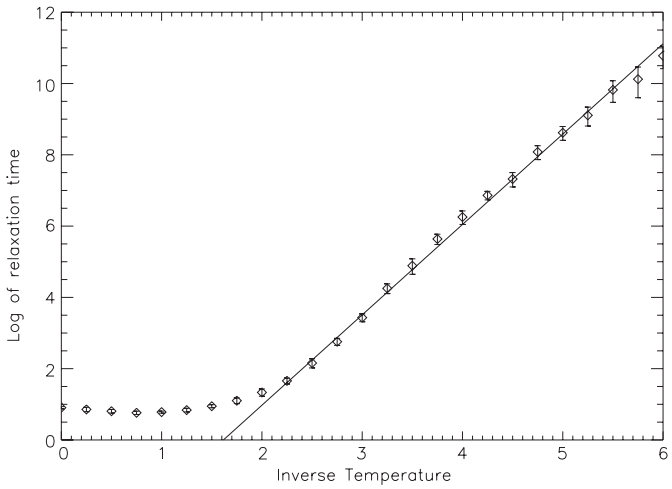

Figure 8. The logarithm of τ_r against inverse temperature. The solid line is an Arrhenius law of the form $\tau_r = 0.0166\, e^{2.535/T}$.

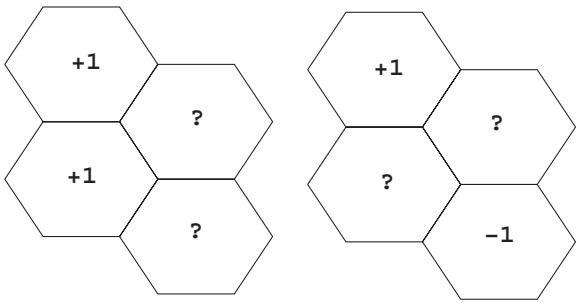

Figure 9. 'Stuck' configurations. On the left, one sees that two spins of +1 adjacent to each other are unable to be flipped within the isolated cluster, regardless of what values the other two spins take (and similarly for two adjacent spins of −1). On the right, we see that two next-to-nearest neighbours of opposite spin cannot be flipped, regardless of the values of the other two spins. A favourable configuration external to the cluster can provide an opportunity to 'unstick' these cells.

due to diffusion of the dimers, and slow dynamics due to movement of the isolated or stuck defects through absorption/creation of dimers. As noted earlier, the former is temperature-independent as dimer diffusion costs no energy; however, the position of the plateau and the subsequent departure from it is dependent on temperature. In particular, the depth of the drop to the plateau from the initial $C(t = 0) = 1$ is determined by the equilibrium concentration of spins of ± 1 in local configurations that are free to move with no change to the energy (these local configurations include the dimers). One can therefore suggest that $C(t)$ might be a sum of two functions in the following way:

$$C(t) = \alpha f(t, \tau_1) + (1 - \alpha) g(t, \tau_2) \tag{9}$$

where α and τ_2 are functions of T, but τ_1 is a constant, and α is the height at which one would expect to find a plateau. f and g are functions to be determined, but they must be monotonically decreasing functions of t, satisfying $f(0, \tau_1) = g(0, \tau_2) = 1$ and $f(\infty, \tau_1) = g(\infty, \tau_2) = 0$.

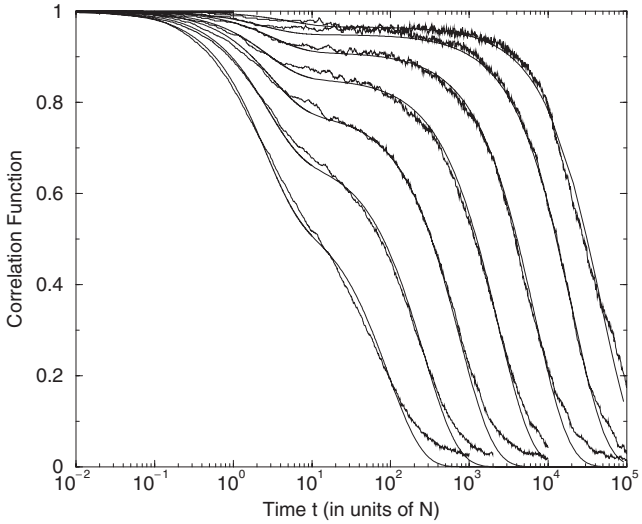

Figure 10. Correlation functions for, from left to right, $\beta = 3, 3.5, 4, 4.5, 5, 5.5, 6$. The solid curves superimposed are the best fits of the form $C(t) = \alpha e^{-t/\tau_1} + (1-\alpha)e^{-t/\tau_2}$.

We tried to fit equation (9) to the data using exponentials for both f and g such that $C(t)$ is of the following form:

$$C(t) = \alpha e^{-t/\tau_1} + (1-\alpha)\, e^{-t/\tau_2}. \tag{10}$$

The results are shown in figure 10; in order to fit more accurately, the system size has been increased to $N = 160\,000$. The fit is extremely good at high values of β (low temperature), although at lower values there is some deviation. We also note that the fitted form drifts below the data at very low values of $C(t)$; there may be some correction to this form which we have not taken into account. We do not claim that this form is exactly correct; nevertheless, it is a useful approximation that may allow us to separate out the two timescales. Previously we stated that we expect τ_1 to be independent of temperature—figure 11(a) shows that this seems to be the case at low β, although as β increases it becomes harder and harder to fit τ_1 accurately due to the extremely high position of the plateau. We have shown the error bars on a few of the points to give some idea of the difficulty in accurately performing this fit at high β; one can see that it is impossible to say anything sensible about the functional form of $\tau_1(\beta)$ for $\beta > 4.5$. However, the naive theory as discussed earlier in connection with $E(t)$ gives $\tau_1 = 2$ and the data is in general accord.

We turn now to τ_2 and consider the dominant processes involved in relaxation in the β-relaxation regime. These are, as previously mentioned, absorption and creation of dimers. Creating a dimer costs 2 units of energy. Each dimer will rapidly diffuse freely through the system until it is absorbed by a defect; this happens quickly as it is an energetically favourable process. Therefore we have energy barriers of 2 and probabilistic barriers of 2β in this regime. Absorption of pre-existing dimers also has a characteristic timescale of $\sim e^{2\beta}$ as the fraction of cells occupied by dimers scales as $e^{-2\beta}$. This is reflected in the behaviour of the second timescale τ_2 as shown in figure 11(b): τ_2 exhibits the Arrhenius behaviour of $\tau_2 = Ae^{B\beta}$, with $B = 2.12$. We have shown error bars on a few of the points; these tend to suggest that the value of B is not exactly 2; however, it is encouraging for the value to be so close given that this is a very crude theory.

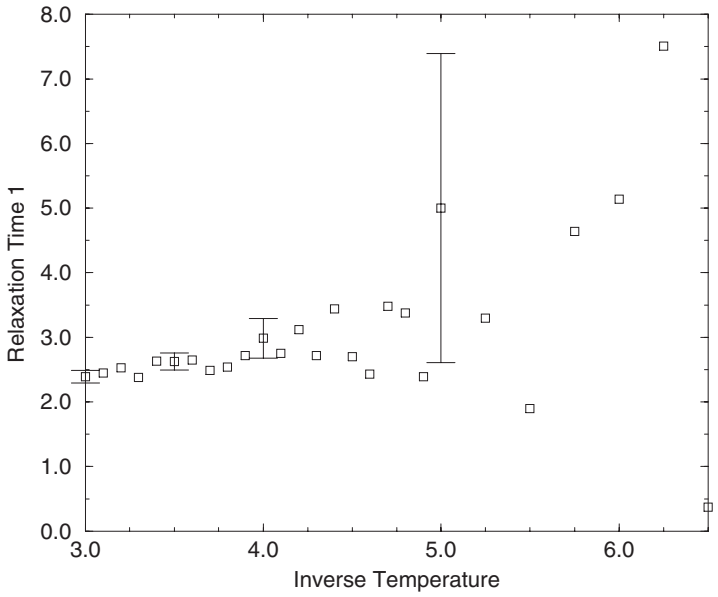

(*a*)

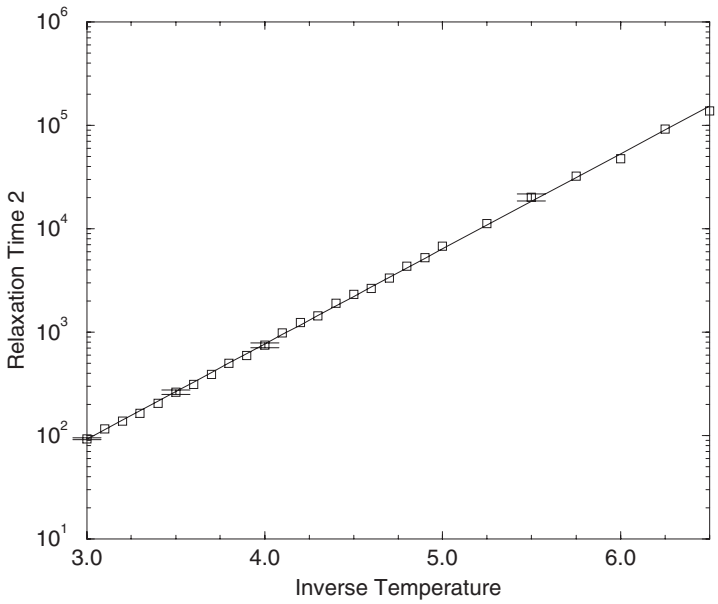

(*b*)

Figure 11. The behaviour of the fitting parameters τ_1, τ_2 and α with temperature; obtained by fitting $C(t) = \alpha e^{-t/\tau_1} + (1-\alpha)e^{-t/\tau_2}$. (*a*) τ_1 against inverse temperature. (*b*) τ_2 against inverse temperature; the superimposed line is $y = Ae^{B\beta}$, where $B = 2.12$. (*c*) (next page) α against inverse temperature; the superimposed curve is $y = \frac{12e^{-\beta}}{(1+2e^{-\beta})^3}$.

The plateau parameter α, is somewhat more complicated. As noted earlier, the initial fast decay of the correlation function is dominated by all the local configurations that can move

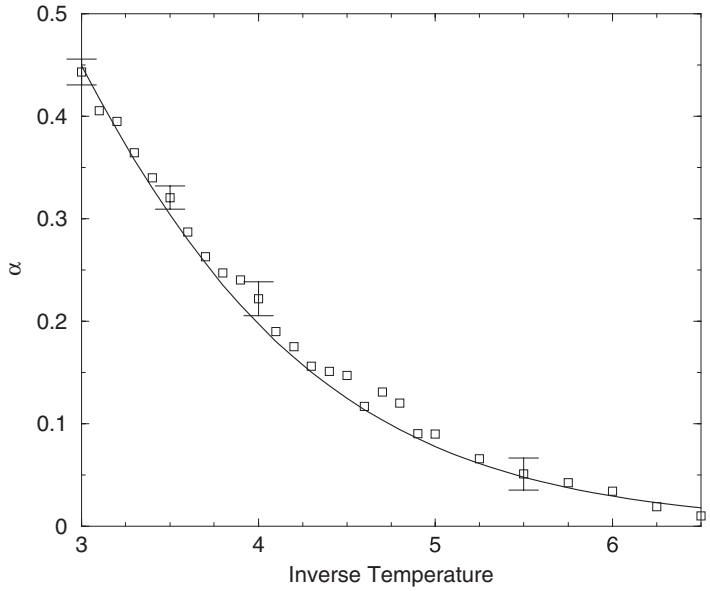

(*c*)

Figure 11. Continued

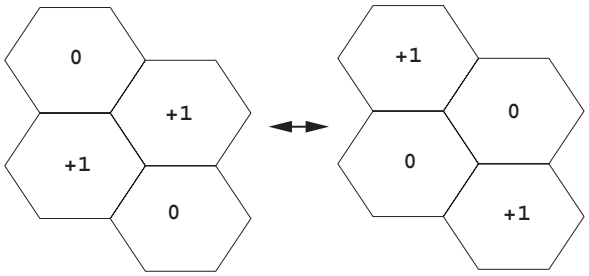

Figure 12. Zero-energy moves for oscillating +1 like-pairs. An identical configuration exists for −1 like-pairs.

freely, without any energy costs. Thus we expect the plateau height to occur roughly at a value of 1 minus the fraction of total spins which can move freely in equilibrium conditions. This fraction contains the dimers, but also certain configurations of like-pairs (i.e. +1, +1 and −1, −1) which can oscillate, as shown in figure 12, although they cannot delocalize without interacting with dimers. In equilibrium the probability that a given defect is part of a +1, −1 dimer is

$$6p(1)p(0)^2 = \frac{6\mathrm{e}^{-\beta}}{(1+2\mathrm{e}^{-\beta})^3} \tag{11}$$

where $p(s)$ is the probability of a spin of value s (the factor 6 comes from the fact the second defect may be situated on any of the six nearest neighbours to the original defect). The probability that any given defect is part of an oscillating like-pair is given by $12p(1)p(0)^2$ (the factor 12 is because there are 12 positions at which the second defect may be situated to make up an oscillating like-pair). However, subsequent to $t = 0$ one supposes that at any instant

in time half of the oscillating like-pairs will be in exactly the same position as at time $t = 0$, and the other half will be in the alternative position. All other processes which cost no energy involve at least three defects, and thus are suppressed in comparison by factors of e^{β} or $e^{2\beta}$. As we are investigating the region of $\beta > 2.5$, we neglect those, and simply suggest

$$\alpha(\beta) = \frac{12e^{-\beta}}{(1 + 2e^{-\beta})^3}. \tag{12}$$

Figure 11(*c*) shows this predicted curve of α against the simulation results for fitting with a sum of two exponentials, from which good agreement can be seen. Therefore for all three parameters (τ_1, τ_2, α) the results of the simulations provide some support to the theory of the dominant processes involved in the evolution of this system.

Note that the relaxation behaviour of the equilibrium correlation function $C(t)$ differs from that of $E(t)$ in two important respects. One is that for $C(t)$ the system is always in macroscopic equilibrium so that the macroscopic distribution of non-zero spins fluctuates around a constant value throughout the dynamics, and all the observed results are due to re-arrangements of the location of these non-zero spins, i.e. annihilations are balanced by creations on a macroscopic level. The second is that one has merely to move a non-zero spin in order to affect $C(t)$, whilst for $E(t)$ to decay from the infinite temperature starting configuration one must actually annihilate ± 1 spins overall.

3.3. Response and overlap functions

We continue to show that this simple spin model behaves in the same fashion as the topological froth by studying response functions in relation to the fluctuation–dissipation ratio. Again we concentrate on the single-site (averaged) case, for which we require the linear response at a site to an infinitesimal perturbation field at the same site. The system is quenched from $\beta = 1$ to the temperature required, and then allowed to evolve at that temperature until time t_w when a field of magnitude h and random sign $\epsilon_i = \pm 1$ is applied. Therefore the perturbation to the energy introduced by the field/charge interaction is

$$\Delta E(t) = h \sum_{i=1}^{N} \epsilon_i s_i(t) \theta(t - t_w) \tag{13}$$

where $\theta(t - t_w)$ is the Heaviside function: $\theta(t - t_w) = 1 \forall t \geqslant t_w$; 0 otherwise. h is a carefully chosen compromise which gives both linear response and a reasonable signal-to-noise ratio. The quantity which one measures is then the linear response function $G(t_w, t_w + t)$:

$$G(t_w, t_w + t) = \frac{\sum_{i=1}^{N} \epsilon_i s_i(t_w + t)}{h \sum_{i=1}^{N} s_i^2(t_w)}. \tag{14}$$

One expects a parametric plot of $-TG(t_w, t_w + t)$ against $C(t_w, t_w + t)$ to have a slope of -1 where the equilibrium fluctuation–dissipation ratio is upheld. Breaking of this conventional equilibrium ratio is characteristic of ageing in glasses [28, 29]; the form of the slope when it is broken provides some information about the nature of the system.

Figure 13 shows the results at various temperatures: these show the same features as the topological froth, namely a breakdown of the fluctuation–dissipation relation when t_w is too short for equilibration to have occurred (for $t_w \to \infty$ the system is already in equilibrium when the perturbation is introduced and FDT holds) and a reduction in the magnitude and an eventual change in sign of the slope as t increases and the correlation function decreases. The non-monotonicity is a consequence of the existence of an absorbing equilibrium state: competition exists between the field, which encourages the non-zero spins to settle on energetically

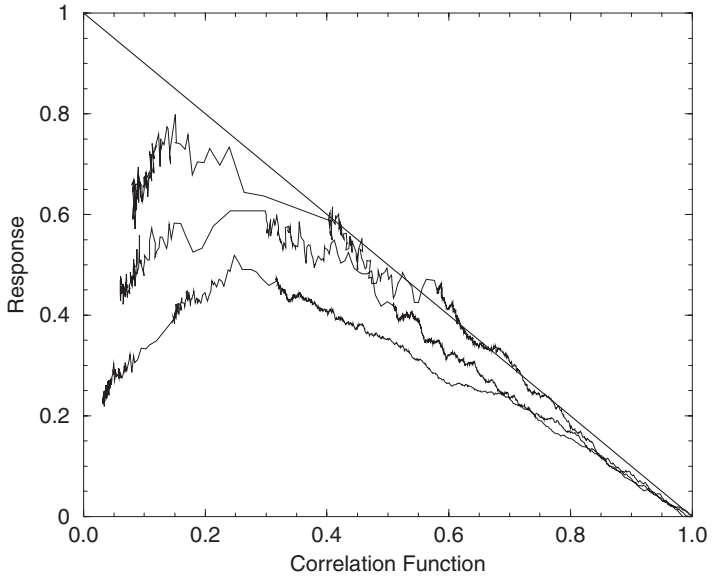

(*a*)

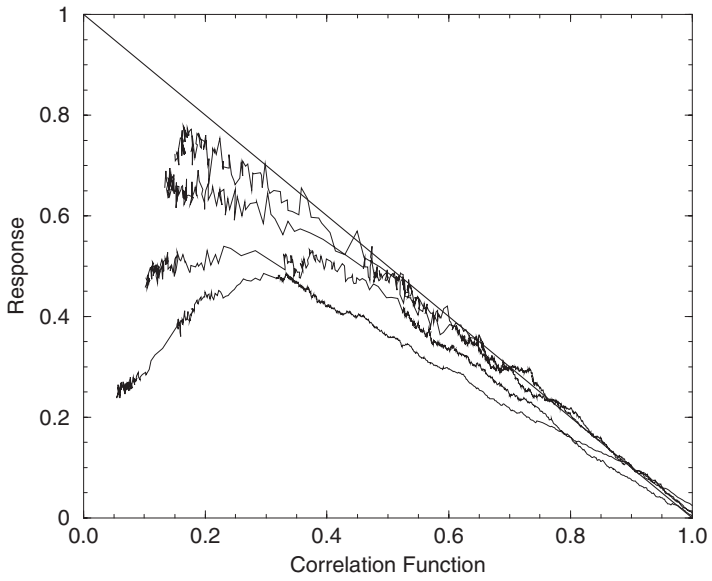

(*b*)

Figure 13. Parametric plots of the response function against the correlation function (each averaged over ten realizations of the charge distribution). (*a*) $\beta = 4$. From lower curve to upper curve, $t_w = 10N, 10^2N, 10^3N$. The straight line of slope -1 is shown for comparison. (*b*) $\beta = 5$. From lower curve to upper curve, $t_w = 10N, 10^2N, 10^3N$ and 10^4N. The straight line of slope -1 is shown for comparison.

favourable sites and thus increases the response, and the natural relaxation to equilibrium, which removes non-zero spins altogether thus reducing the response (one should recall that spins of value 0 make no contribution whatsoever to the response). At time t_w (that is for $t = 0$)

when the field is switched on, the response is on average zero. If t_w is short enough that the fast processes remain dominant (i.e. $E(t_w)$ has not yet reached the intermediate plateau) then these energetically favourable fast moves are quickly carried out. This simultaneously removes many non-zero spins, and also settles many non-zero spins on energetically favourable sites; the former process does not on average decrease the response since at t_w it is zero on average anyway, and the latter process increases the response. Once the dimer concentration has relaxed to the equilibrium level (i.e. after the onset of the plateau in $E(t_w + t)$) the response increases more slowly as the evolution of the system is dominated by the movement of isolated defects, which occurs on much longer timescale. The applied field causes these isolated defects to tend to settle on energetically favourable sites; however, as time passes they will be removed from the system until the equilibrium concentration is reached. Therefore one expects the response to peak before settling at a finite value once equilibrium has been reached (the final value reached is dependent on the waiting time t_w through the normalization of both the response and the correlation functions).

In order to distinguish between different types of ageing, Barrat, Burioni and Mezard suggested the study of the overlap $Q_{t_w}(t)$ between two replicas [30]. These replicas are identical configurations at time t_w, but are subsequently evolved according to different stochastic thermal noise (but of the same characteristic temperature), with $Q_{t_w}(t)$ of the form

$$Q_{t_w}(t) = \frac{\sum_{i=1}^{N} \sigma_i^1(t_w + t)\sigma_i^2(t_w + t)}{\sum_{i=1}^{N} \left(\sigma_i^1(t_w)\right)^2} \tag{15}$$

where σ is some order parameter of the system and the superscripts 1, 2 refer to replicas 1, 2. Barrat *et al* classify systems as either Type I or Type II models: for the former, the appropriate $Q_{t_w}(t)$ (normalized to 1 at time $t = 0$) decays to a finite, non-zero value in the double limit $\lim_{t_w\to\infty} \lim_{t\to\infty} Q_{t_w}(t)$; this class includes models which are dominated by coarsening (for a review of coarsening see [31]). For the class of Type II, $Q_{t_w}(t)$ decays to zero in this limit; this class includes glassy systems [7]. In equilibrium (i.e. t_w greater than the equilibration time of the system) there is no t_w dependence so $Q_{t_w}(t) = Q(t)$; one also finds that $Q(t) = C(2t)$ (for details see [30]).

For this model, the overlap we use is as given in equation (15) with $\sigma_i = s_i$. We start from non-equilibrium conditions, where the system is quenched at $t = 0$ from $\beta = 1$ to the temperature in question, and then allowed to run at that temperature until time t_w when measurements commence. In figure 14 we show the overlap and $C(t_w, t_w + 2t)$ against time for $\beta = 5$; initially Q is almost identical to $C(t_w, t_w + 2t)$, but it drops below $C(t_w, t_w + 2t)$ at longer times. For larger values of t_w this takes longer to happen since these systems start off closer to equilibrium. We also show the equilibrium curves, for which $Q(t) = C(2t)$.

Given that $Q(t) = C(2t)$ in equilibrium, we can check our proposed functional form for the equilibrium correlation function through a parametric plot of the overlap against $C(t)$. If $C(t)$ is indeed of the form given in equation (10) then one expects

$$Q(t) = C(2t) = \alpha e^{-2t/\tau_1} + (1 - \alpha)e^{-2t/\tau_2}. \tag{16}$$

Thus for long times one would expect to find

$$Q(t) \sim (1 - \alpha)e^{-2t/\tau_2} \sim \frac{C(t)^2}{(1 - \alpha)} \tag{17}$$

and for short times

$$Q(t) \sim \alpha e^{-2t/\tau_1} + (1 - \alpha) \sim \frac{(C(t) + \alpha - 1)^2}{\alpha} + (1 - \alpha). \tag{18}$$

Figure 15 shows parametric plots of the overlap $Q(t)$ against the correlation function $C(t)$ (in equilibrium) for different values of β. These plots should be 'read' from the top right

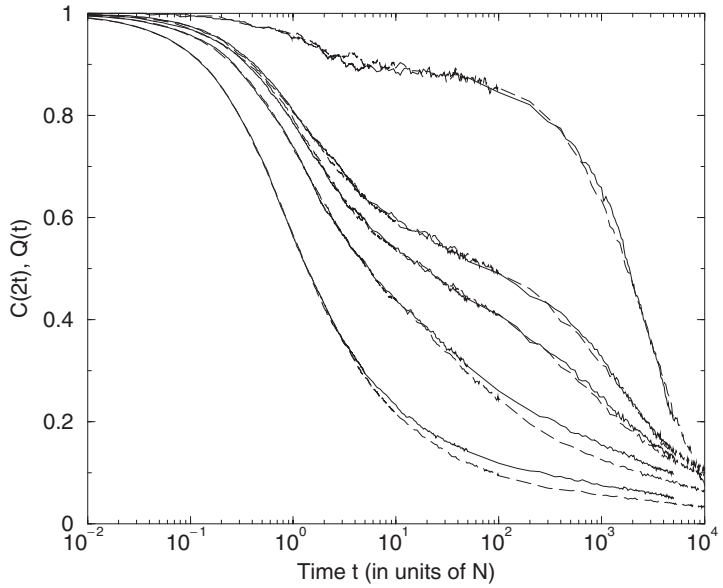

Figure 14. The behaviour of $C(t_w, t_w + 2t)$, $Q_{t_w}(t)$ with time for $\beta = 5$. $Q_{t_w}(t)$ is given by the dashed curves and $C(t_w, t_w + 2t)$ by the solid curves. From lower curve pair to upper curve pair, $t_w = 10N, 10^2N, 10^3N, 10^4N$. The uppermost pair is that of equilibrium, with $Q(t) = C(2t)$.

corner, i.e. $t = 0$ occurs when $Q(t) = C(t) = 1$, and long times correspond to low values of $Q(t), C(t)$. We have plotted on each the expected short-time and long-time behaviour as given in equations (17) and (18), where the values of α are those fitted in the previous section. One sees that the short-time expression fits the data extremely well, supporting our hypothesis that the initial decay of the correlator, from 1 down to the plateau, is exponential. The longer time behaviour initially fits very well for both $\beta = 4$ and 5 (figures 15(a) and (b)), although as time goes on the theoretical curve drops below the data. This tends to suggest that at long timescales there is some correction to this fitted form which we have not taken into account; the second relaxation may be some kind of modified exponential rather than pure exponential. For the case of $\beta = 3$ (figure 15(c)) the values of τ_1, τ_2 are much closer together and thus the two timescales are not so well separated. Therefore one does not see a well-defined plateau in the equilibrium correlation function (see figure 7(a)), and the cusp in this parametric plot is also not as clear. The cusp in these plots is a direct result of the existence of the plateau; since $Q(t) = C(2t)$ in equilibrium, the overlap function $Q(t)$ reaches the plateau before the correlator $C(t)$. Thus there is a time period for which $Q(t)$ is effectively stationary whilst $C(t)$ is still dropping fast. This is followed by a time period for which the plateaux in both functions overlap, and therefore both are stationary, and then there is a regime in which $Q(t)$ drops away from the plateau whilst $C(t)$ is still stationary. This tells us that whilst the dominant process is diffusion of the dimers, the two copies of the system are restricted to a narrow area of phase space; this is because the isolated defects have not yet moved in either copy, and thus the overlap will be high. It is only once the activated processes become dominant that the two copies can move well apart from each other.

Figure 16 shows a parametric plot of the overlap against the correlator for the non-equilibrium case, i.e. $Q_{t_w}(t)$ against $C(t_w, t_w+t)$. The initial behaviour is independent of t_w and in fact follows the short-time behaviour we expect in equilibrium. However, as $C(t_w, t_w + t)$

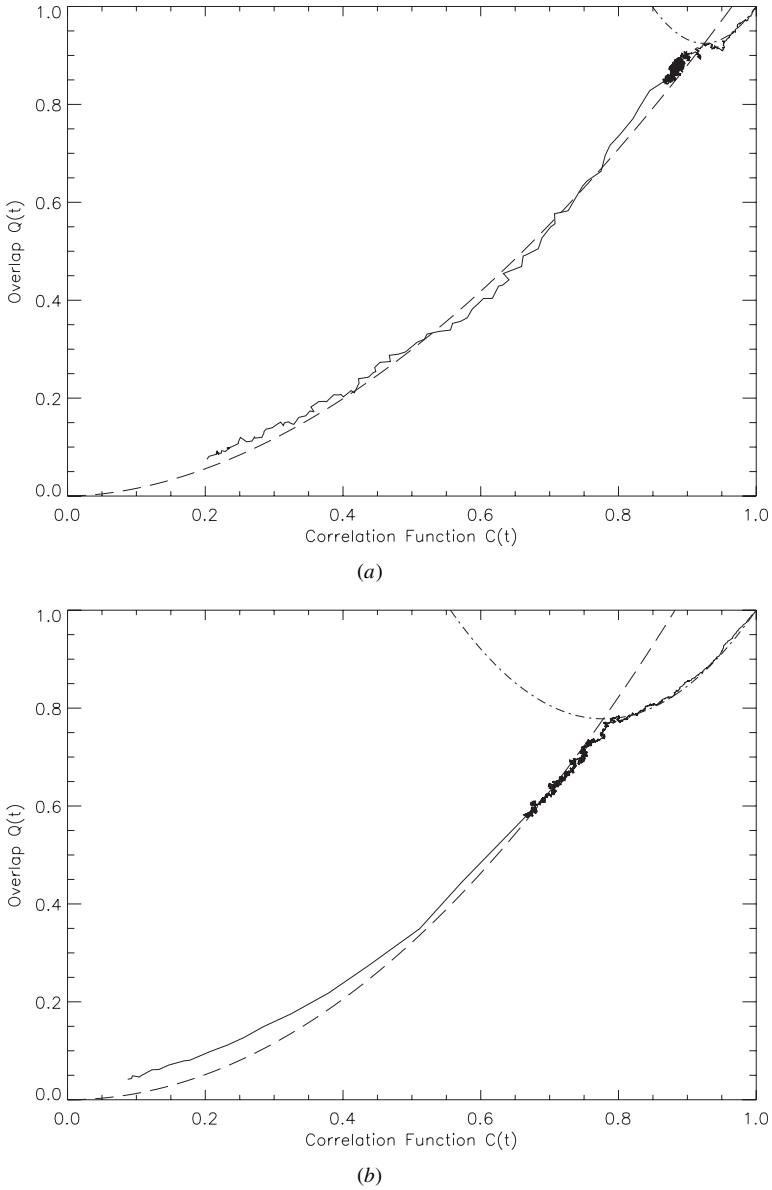

(*a*)

(*b*)

Figure 15. The overlap function $Q(t)$ against the correlation function $C(t)$. In each case the dot-dashed curve is the expected short-time behaviour and the dashed curve is the expected long-time behaviour, if equation (10) holds. The values of α are those fitted in the previous section.(*a*) $\beta = 5$, $\alpha = 0.0899$. (*b*) $\beta = 4$, $\alpha = 0.222$. (*c*) (next page) $\beta = 3$, $\alpha = 0.447$.

drops below 0.9, the curves fall below the equilibrium behaviour and we see evidence of dependence on t_w. The cusp that develops is sharper for larger t_w, with the behaviour tending towards that of equilibrium. For the smaller values of t_w there is no channelling in phase space because the starting configuration is well away from equilibrium, and thus there are many different energetically favourable routes to be taken. It is clear from these figures that our model falls into the class of Type II, as the overlap decays to zero rather than a finite value as

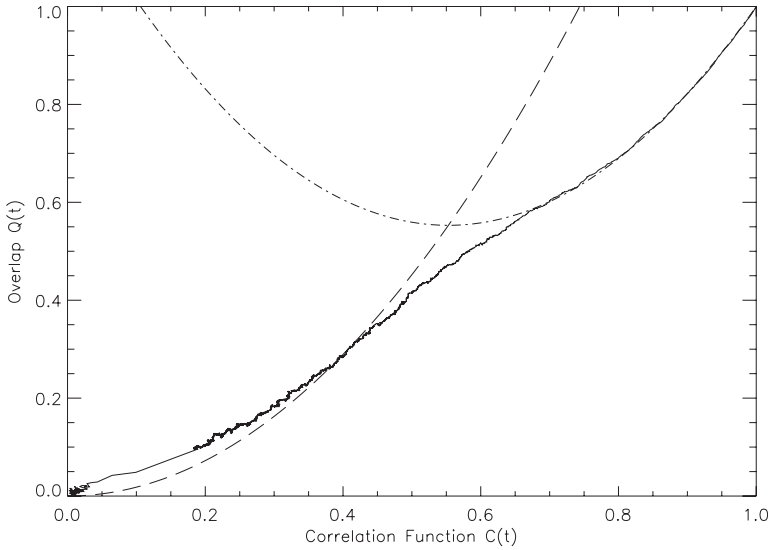

(*c*)

Figure 15. Continued

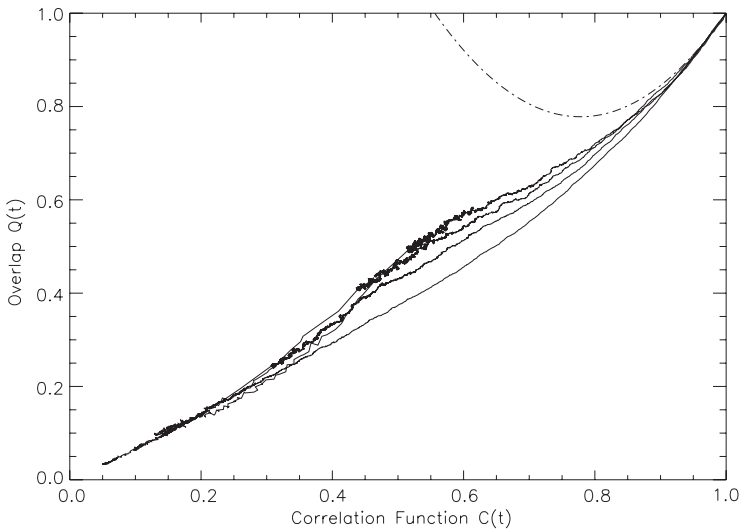

Figure 16. $Q_{t_w}(t)$ against $C(t_w, t_w + t)$ for $\beta = 4$. From lower to upper curve, $t_w = 10N, 10^2N, 10^3N, 10^4N$. The dotted curve is that of expected short-time behaviour for $Q(t)$ against $C(t)$ in equilibrium.

it would do for Type I systems; this is as expected as we believe our model to be glassy rather than dominated by coarsening.

To summarize our findings so far, we have shown that the $D > 0$ model does indeed give results that are quantitatively similar to those of the topological model, whilst having the advantage of being simpler, computationally faster and more suited to analytic study. We have developed a conceptual picture involving both fast and slow dynamics, and many of the features of this model can be described in terms of this picture. We find good agreement

between theoretical predictions and data for the behaviour of the correlation function, energy and overlap function.

4. $D < 0$

4.1. Relaxation dynamics and correlation functions

We shall now turn our attention to the model with $D < 0$, setting $D = -1$. Unlike the previous case, this model does not have a unique absorbing ground state; instead, there are a great many degenerate ground states, although some of these are not accessible using our dynamical rules. This raises the possibility that in preparing an 'equilibrium' system by randomly placing throughout the lattice the correct number of ± 1's for that temperature, one might pick out an inaccessible configuration. However, the probability of this occurring is so small as to be negligible, and we have checked that the results obtained by this method do not differ from those obtained through waiting long enough for equilibration to occur. Thus when we refer to an equilibrated system, we mean one that has been prepared through a random allocation of the correct number of non-zero spins.

We expect the $D < 0$ model to also show glassy behaviour with two different timescales, but as the system now favours $s_i = \pm 1$ rather than $s_i = 0$, the equivalent of the free-moving dimers will be fast-moving pairs of spin zero, and the analogue of the slow-moving energetically trapped defects will be isolated zero-spins. With the correct choice of observables, one expects to see all the same features as with the $D > 0$ model. However, although one expects similar qualitative behaviour[3], the quantitative behaviour should be different—this is because $A + A \to \emptyset$ processes replace those of type $A + B \to \emptyset$ and also because the zero-spin dimers cannot move quite so easily through the ± 1 background. As shown in figure 9 there are certain configurations that simply cannot move.

Simulations were again performed for $N = 9900$. Figure 17(a) confirms that we do see glassy behaviour when the system is cooled at different cooling rates. A plot of the energies attained after running for a variety of times t_w at various temperatures T from a starting configuration corresponding to infinite temperature are shown in figure 17(b); the presence of activated processes is indicated by the clear minima and by the plateau at $\frac{E}{N} \sim -0.94$ below which the system cannot penetrate at low temperatures, even after the longest waiting times. Again one can see this plateau clearly in a plot of energy against time subsequent to a quench from infinite temperature (see figure 18(a)); one can again re-scale the time axis to $T \ln t$ in order to see the staircase shape appear (figure 18(b)).

Because the background does not necessarily allow the dimers to move freely, one must consider the possibility that the dimer diffusion may be dependent upon the density of non-zero spins. In equilibrium, this density is dependent upon the temperature; therefore we have investigated the persistence of non-isolated zero-spins under equilibrium conditions. In order to do this, one can identify all zero-spins that have at least one neighbouring spin which is also zero in the starting equilibrium configuration; as the system evolves, one can measure the fraction of these that have NOT been involved in a move. Figure 19(a) shows these results for $D < 0$; one can see that the persistence is weakly temperature dependent. One cannot sensibly investigate the effect at lower temperatures because there are so few zero-spins present in equilibrium conditions. For comparison, we also show the results for the $D > 0$ model, where the persistence is defined as the fraction of non-zero spins with at least one neighbour of the opposite sign that have NOT undergone a move. The results are shown in figure 19(b)

[3] Except in pathological cases.

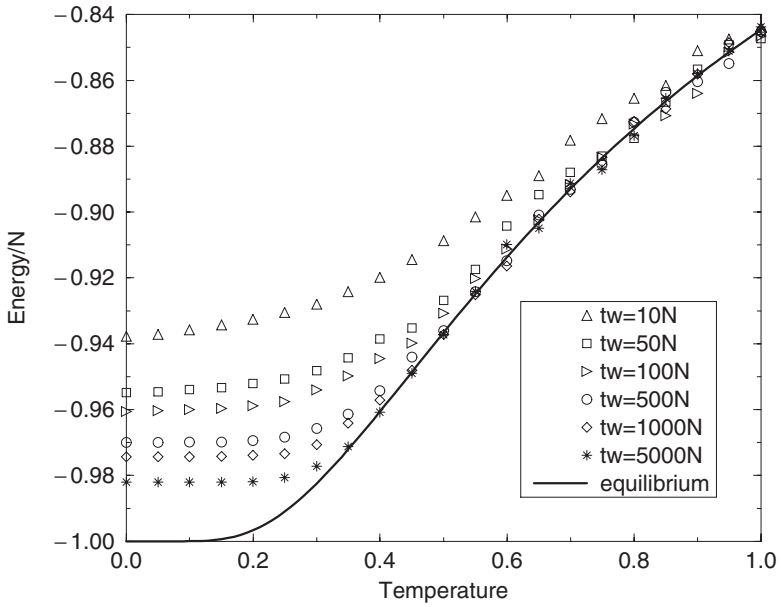

(*a*)

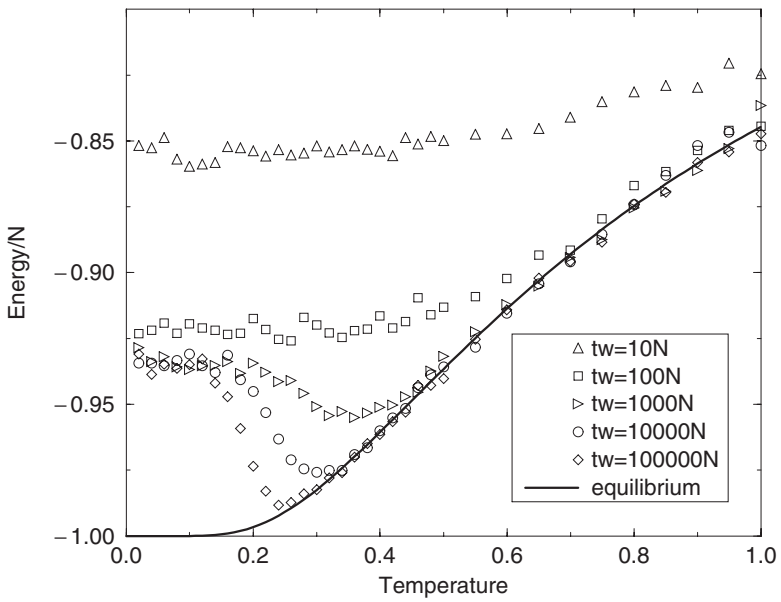

(*b*)

Figure 17. Energy against temperature for slow cooling and rapid quench. (*a*) The behaviour of the energy under cooling ($D < 0$). The values of t_w are the waiting times at each point.(*b*) The behaviour of the energy after a rapid quench ($D < 0$). The values of t_w are the times, subsequent to the quench, at which the energy is measured.

and show no temperature dependence. This result has implications for the form of both the correlation function and the energy.

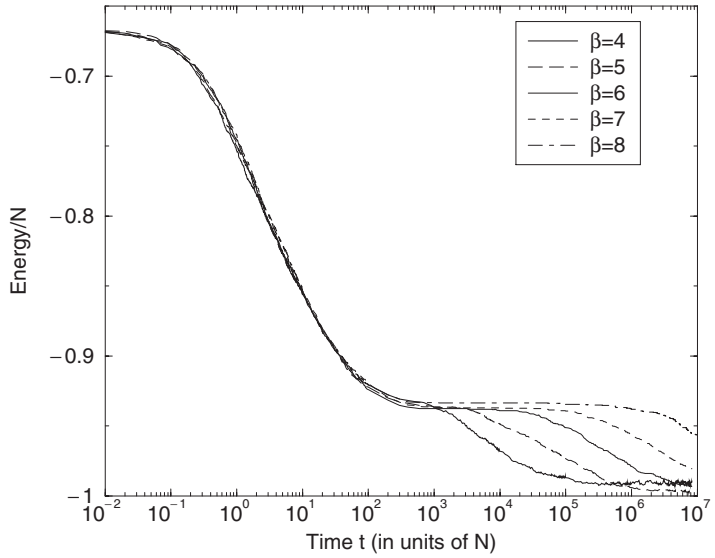

(*a*)

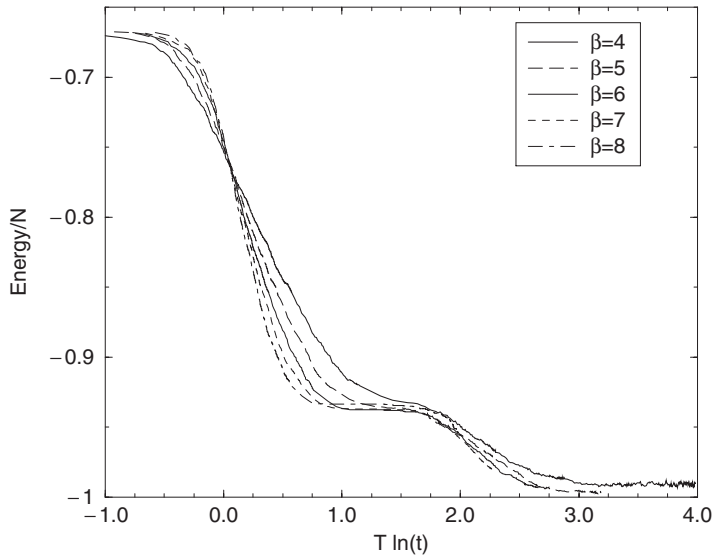

(*b*)

Figure 18. The behaviour of the energy with time. (*a*) Energy against time. (*b*) Energy against $T \ln t$, where t is measured in units of N.

In order to produce a fit for the energy relaxation from a starting configuration corresponding to infinite temperature, one must think very clearly about the processes involved. The initial fast decay to the plateau involves two pairs of zero-spin dimers annihilating; this is of type $A + A \rightarrow \emptyset$, which one expects to give a $t^{-\frac{d}{2}}$ dependence in the energy in the asymptotic limit [18, 19][4]. At this stage the density dependence of the dimer diffusion is not likely to be

[4] In fact the critical dimension $d_c = 2$ for this theory, and one expects logarithmic corrections at this point, but we shall ignore these.

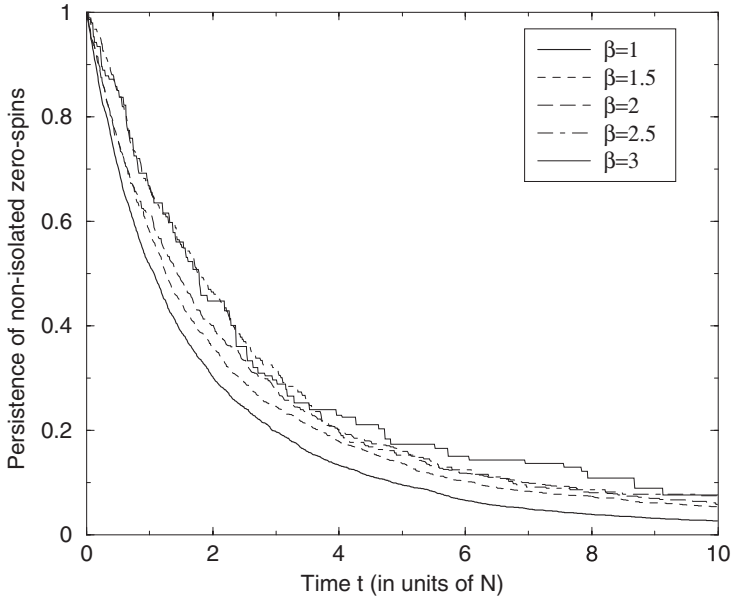

(*a*)

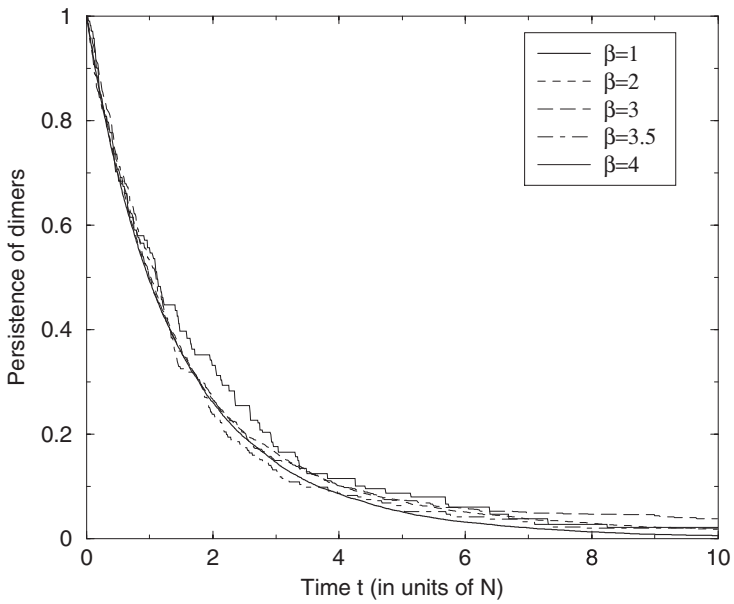

(*b*)

Figure 19. Persistence functions for both $D < 0$ and $D > 0$. (*a*) The persistence of non-isolated zero-spins for $D < 0$. (*b*) The persistence of non-zero spins with at least one opposite neighbour for $D > 0$.

strong enough to cause substantial deviation from the $A + A \rightarrow \emptyset$ behaviour so one expects the initial decay to behave as $(1 + m_1 t)^{-1}$; however, it is not trivial in this case to determine what the value of m_1 might be. Because the zero-spin dimers are not completely free to move

diffusively through the background we are unable to produce an accurate estimate; we simply expect a value of m_1 of the order of 1. For the slow decay from the plateau to equilibrium, the density dependence of the dimer diffusion will have a substantial effect because there are far more ± 1 spins present as the system flows closer to equilibrium. The slow process involves the pairing of isolated zero-spins through the mechanism of dimer creation and absorption; it is unlikely to behave exactly as an $A + A \to \emptyset$ process given that the dimers cannot diffuse freely to facilitate it. One can fit this latter part separately, and one finds it takes the form $a_1(1 + t\mathrm{e}^{-2\beta})^{-\kappa}$; the factor of two in the exponential was fitted as a free parameter and a result of almost exactly 2 was obtained for every temperature. This is in keeping with the energy barrier of 2 involved in creating a dimer. The parameter a_1 is naturally associated with the plateau value and clearly takes a value ~ -0.94. The value of κ is approximately 0.6; this is substantially slower than the behaviour one would find asymptotically with a pure $A + A \to \emptyset$ process and is due to the inhibited movement of the dimers.

Having fitted the latter part, we attempted a fit of the full dataset of the form

$$\frac{E}{N} = \left(-\frac{2}{3} - a_1\right)(1 + m_1 t)^{-\kappa_1} + (a_1 - e_{\mathrm{eq}})(1 + t\mathrm{e}^{-2\beta})^{-\kappa_2} + e_{\mathrm{eq}} \tag{19}$$

where $a_1, \kappa_1, \kappa_2, m_1$ are all parameters to be determined, and e_{eq} is the equilibrium energy per cell at the temperature in question. One cannot fit this well to the data, as shown in figure 4(*a*): the decay is faster than that of a power law in the latter stages of the decay to the intermediate plateau. Thus we must think again about the processes involved in the relaxation of the energy to the plateau.

As mentioned earlier, besides the $A + A \to \emptyset$ fast processes, there is also a fast process involving a dimer interacting with a defect to leave an isolated defect—this is of type $A + C \to \emptyset + C$, and thus typically gives a stretched exponential for the asymptotic behaviour of the energy with time. We did not need to include these in the fit to the energy for $D > 0$; however, it is clear from the poor fit in figure 20(*a*) that in the $D < 0$ case we cannot neglect them. We therefore expect the energy density E/N to be approximated by the following form:

$$\frac{E}{N} = \left(-\frac{2}{3} - a_1\right)(a_2(1 + m_1 t)^{-\kappa_1} + (1 - a_2)\mathrm{e}^{-(m_2 t)^{\nu}}) + (a_1 - e_{\mathrm{eq}})(1 + t\mathrm{e}^{-2\beta})^{-\kappa_2} + e_{\mathrm{eq}} \tag{20}$$

where a_1, κ_2 can be fitted separately from the decay from the plateau to equilibrium, and $a_2, \kappa_1, \nu, m_1, m_2$ are parameters to be determined. The theory would suggest that κ_1 should be close to 1, and that m_1 should be of the order of 1. Figure 20(*b*) shows these fits superimposed on the data; it will be noted that agreement is excellent. The values of the parameters are given in the caption; in particular, one notes that κ_1 is extremely close to 1 in each case, and that m_1 is indeed of the order of 1. We have already discussed the power law decay from the intermediate plateau to equilibrium. Without developing a much more complex theory one can say little about the parameters in the stretched exponential term.

With regards to the correlation function, in order to study the $D > 0$ model we chose a function which focussed on the defects. We do the same in this case, and thus the correlation function we measure is

$$C(t_{\mathrm{w}}, t_{\mathrm{w}} + t) = \frac{1}{1 - p_{\mathrm{eq}}(0)}\left(\frac{\sum_{i=1}^{N} \delta_{s(t_{\mathrm{w}}),0}\delta_{s(t_{\mathrm{w}}+t),0}}{\sum_{i=1}^{N} \delta_{s(t_{\mathrm{w}}),0}} - p_{\mathrm{eq}}(0)\right) \tag{21}$$

where $p_{\mathrm{eq}}(0)$ is the equilibrium density of zero spins at the temperature of interest. The somewhat unusual normalization is necessary to allow the correlation function to decay to zero rather than to a finite value equal to $p_{\mathrm{eq}}(0)$; this finite plateau comes about because a fraction $p_{\mathrm{eq}}(0)$ of the cells that have spin zero at time $t = 0$ can be expected to have spin zero

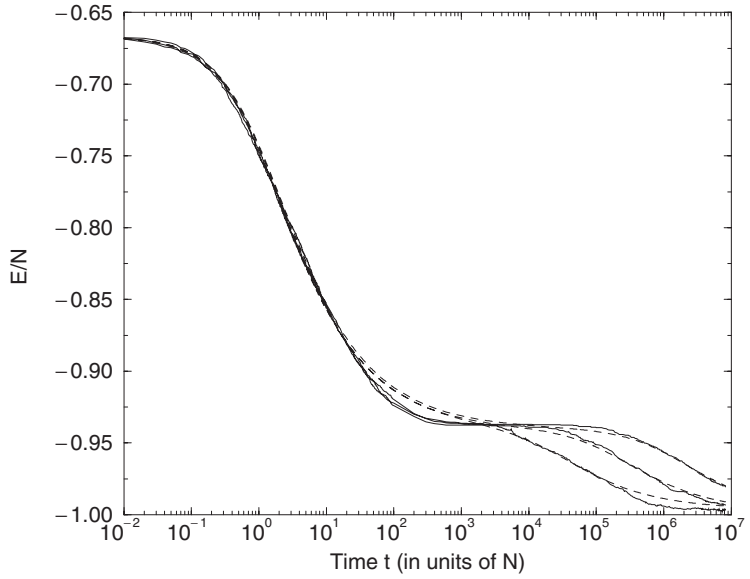

(*a*)

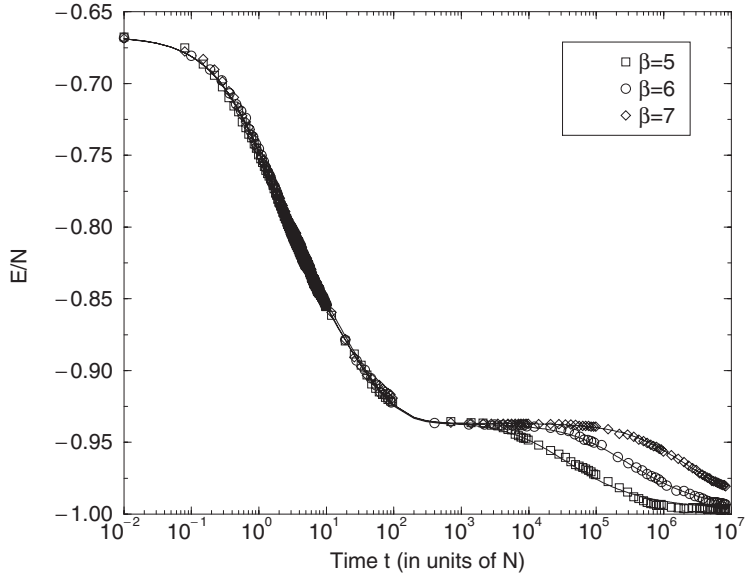

(*b*)

Figure 20. Fits to the energy. (*a*) The energy for (from left to right) $\beta = 5, 6, 7$ fitted with equation (19); the fits are the dashed curves. The parameters $(a_1, m_1, \kappa_1, \kappa_2)$ are as as follows: for $\beta = 5$, $(-0.942, 1.02, 0.49, 0.52)$; for $\beta = 6$, $(-0.941, 0.93, 0.50, 0.51)$ and for $\beta = 7$, $(-0.941, 0.93, 0.49, 0.54)$. (*b*) The energy fitted with equation (20); the fits are the solid curves. $(a_1, a_2, m_1, \kappa_1, m_2, \nu, \kappa_2)$ are as follows : for $\beta = 5$, $(-0.936, 0.61, 0.748, 0.98, 0.0385, 0.638, 0.62)$; for $\beta = 6$, $(-0.937, 0.57, 0.77, 0.977, 0.0389, 0.64, 0.59)$ and for $\beta = 7$, $(-0.937, 0.66, 0.46, 1.0, 0.0313, 0.474, 0.59)$.

at any later time. In the $D > 0$ model, we did not have to take into account this effect since the contribution from spins that remain +1 (or -1), and those that swap from +1 to -1 (or -1

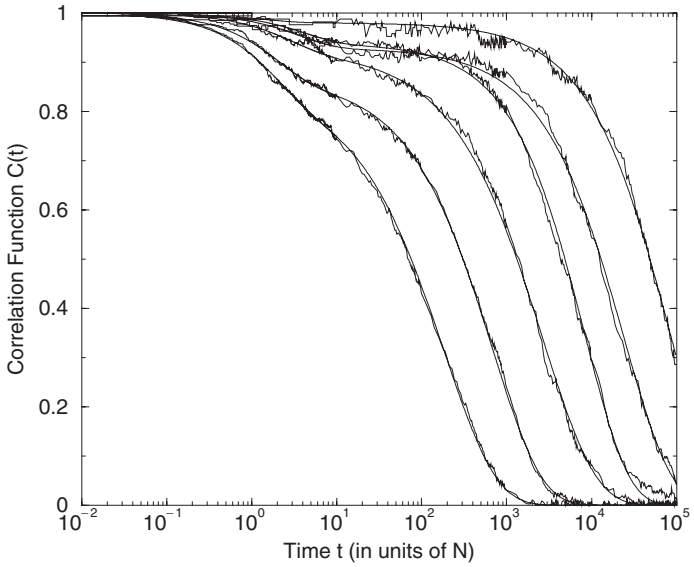

Figure 21. Correlation functions in equilibrium conditions. From left to right, $\beta = 2.5, 3, 3.5, 4, 4.5, 5$. The superimposed fits are of the form $C(t) = \alpha e^{-t/\tau_1} + (1-\alpha)e^{-(t/\tau_2)^\gamma}$.

to +1) cancel out. Figure 21 shows that this function does indeed produce similar results to those of the $D > 0$ model: again, we can see clear evidence of two-step relaxation. The fits superimposed upon the data are of the following form:

$$C(t) = \alpha e^{-t/\tau_1} + (1-\alpha)e^{-(t/\tau_2)^\gamma}. \tag{22}$$

It will be noted that these fits are extremely good, and also that the relaxation in the long-time region follows a stretched exponential rather than an exponential as in the $D > 0$ case. This is a result of the temperature dependence of the dimer diffusion, which slows the decay from the plateau. Thus γ in figure 22(d) is less than one in all cases. We do not have a full theory of the behaviour of the system in this region and thus cannot comment further on the behaviour of this exponent.

One might naively expect the predicted value of τ_1 to be altered by the fact that the zero-spin dimers are not necessarily free to move through the ± 1 background. In fact this is not the case: τ_1 is the timescale for the dimers that are *free to move* only, and we can still expect those free dimers to move with a timescale of 2, independent of temperature, exactly as in the $D > 0$ case. Figure 22(a) shows the values of τ_1 against inverse temperature obtained from fitting the correlation functions with equation (22)—this data is in keeping with a temperature-independent value of $\tau_1 = 2$. Those dimers that are not free to move do not contribute to the initial fast decay of the correlation function. The parameter that the extra jamming *does* alter is α: one expects the correlation function to decay to a plateau value which is one minus the density of free zero-spins (although one must remember to normalise correctly as in equation (21)). Thus we have to calculate the probability of obtaining a zero-spin dimer which can move (shown in figure 4(c), but one should now think of the ± 1 as being the background and the zero-spins as being the dimer), and also of obtaining a zero-spin pair which can oscillate (as in figure 12). This gives a probability of $24p(0)p(1)^2$; thus after normalisation, we expect α to behave as

$$\alpha = \frac{12e^{\beta}}{(1+2e^{\beta})^2} - \frac{e^{-\beta}}{2}. \tag{23}$$

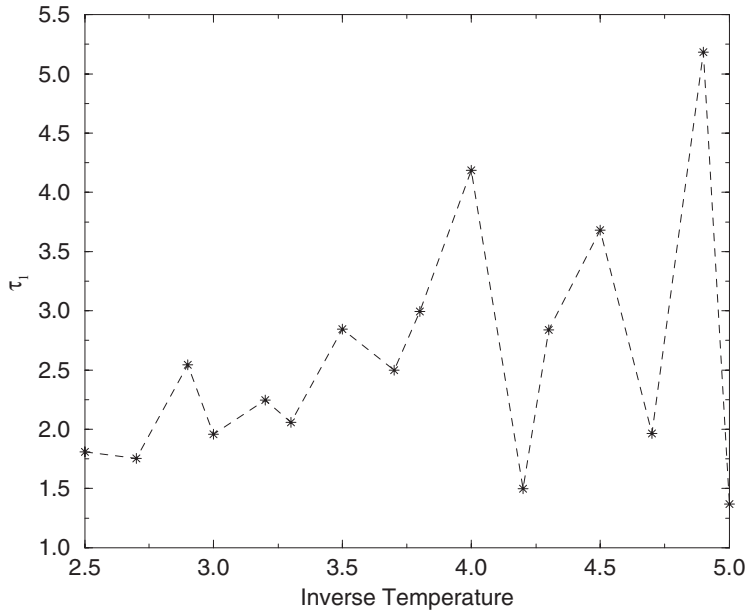

(*a*)

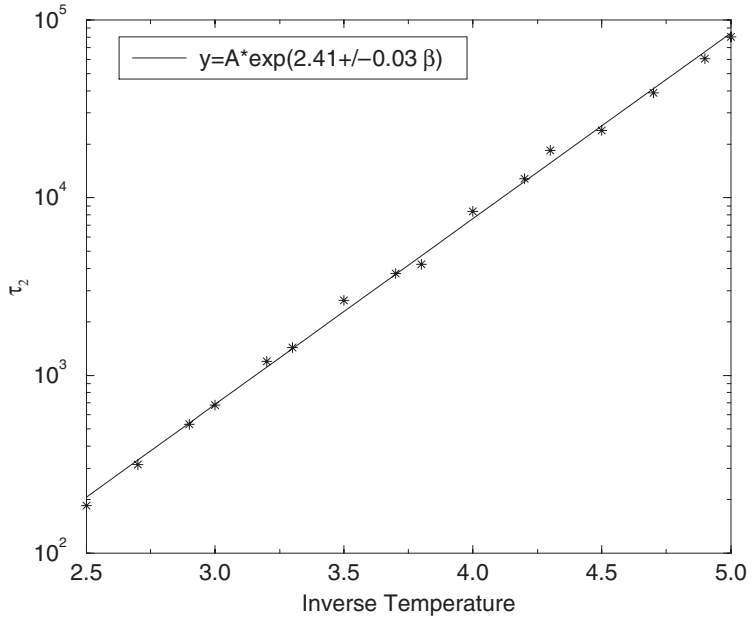

(*b*)

Figure 22. The behaviour of the fitting parameters α, τ_1, τ_2 and γ with temperature. The data was obtained by fitting the form $C(t) = \alpha e^{-t/\tau_1} + (1-\alpha)e^{-(t/\tau_2)^{\gamma}}$ to the equilibrium correlation functions. (*a*) τ_1 against inverse temperature. (*b*) τ_2 against inverse temperature. (*c*) (next page) α against inverse temperature; the superimposed curve is $y = \frac{12e^{\beta}}{(1+2e^{\beta})^2} - \frac{e^{-\beta}}{2}$. (*d*) γ against inverse temperature.

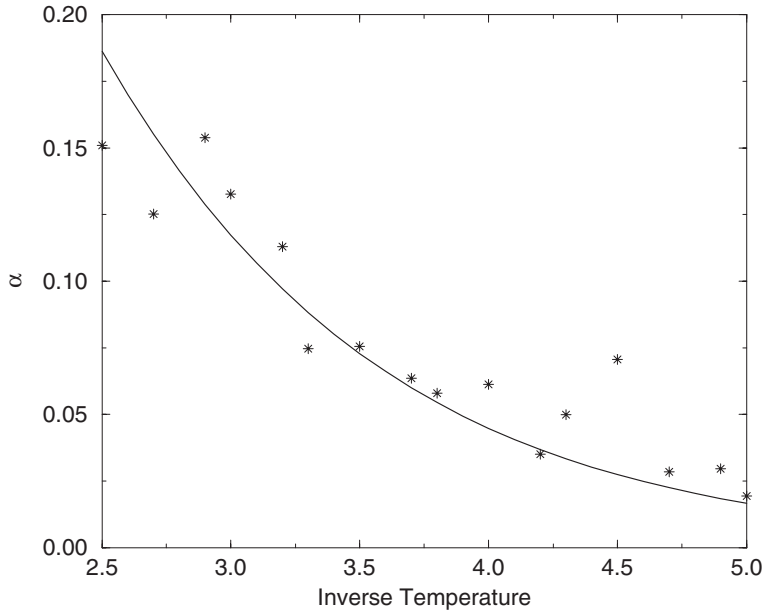

(*c*)

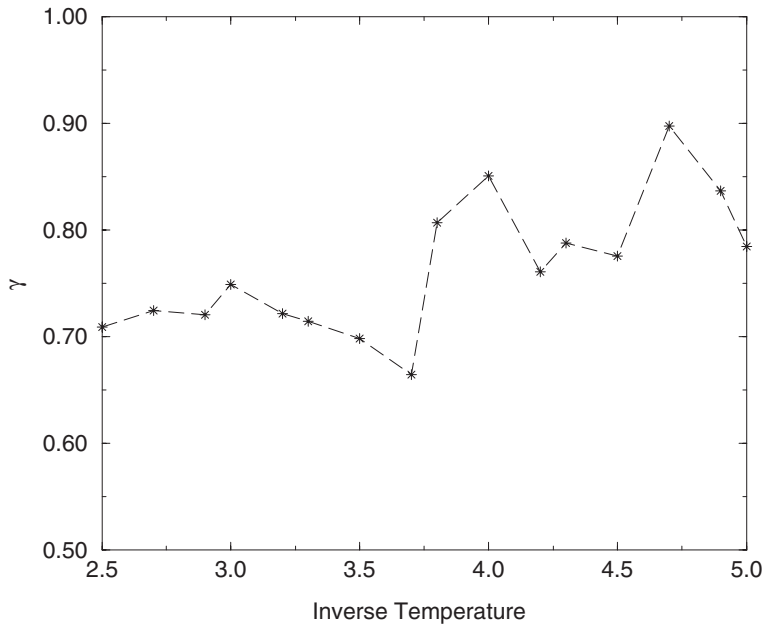

(*d*)

Figure 22. Continued

Figure 22(*c*) shows this curve superimposed upon the fitted values of α against temperature; the data shows reasonable agreement with the theory.

One can see from figure 22(*b*) that we again observe Arrhenius behaviour for τ_2. In this case, however, the best-fit Arrhenius law is $\tau_2 \sim e^{2.4\beta}$, whereas the energy barrier argument

would suggest $\tau_2 \sim e^{2\beta}$. As mentioned earlier, we lack a full understanding of the behaviour in this region, and can only say that this discrepancy is probably also due to the fact that the ± 1 background does not allow the zero-spin dimers to diffuse freely.

4.2. Response and overlap functions

We continue our study of the $D < 0$ model by observing the response of the system to an applied field. As before, a field $h\epsilon_i$ is applied at time t_w, with $\epsilon_i = \pm 1$ randomly at each site. The perturbation this introduces to the energy is $\Delta E(t) = h \sum_{i=1}^{N} \epsilon_i \delta_{s(t),0}\, \theta(t - t_w)$, where $\theta(t - t_w)$ is again the Heaviside function. The observable we then measure is the following linear response function: $G(t_w, t_w + t)$:

$$G(t_w, t_w + t) = \frac{1}{h(1 - p_{eq}(0))} \left(\frac{\sum_{i=1}^{N} \epsilon_i \delta_{s(t_w+t),0}}{\sum_{i=1}^{N} \delta_{s(t_w),0}} \right). \tag{24}$$

Again one expects a parametric plot of $-TG(t_w, t_w+t)$ against the correlation function (defined as in equation (21)) to yield a slope of -1 where the conventional FDT is upheld.

Figure 23 shows such a parametric plot for a variety of temperatures and waiting times t_w. One can see the main features of the equivalent $D > 0$ plots in these figures: FDT is upheld for a time which increases as t_w increases, and sometime after it is broken the curves display non-monotonic behaviour. As in the $D < 0$ case, this turnover in the response after long times (i.e. low values of the response and of $C(t_w, t_w + t)$) is due to the isolated defects being eliminated from the system, thus decreasing the response. Note that although this turnover can been seen clearly in figure 23(*a*), one cannot always run the simulations for long enough to observe this effect at low temperatures and large waiting times; in fact, it is not observable for any waiting times for $\beta = 6$ (figure 23(*c*)). However, in addition to this behaviour, at very low temperatures and for short t_w we see an intermediate 'hump' appearing before the turnover due to the isolated defects—see figures 23(*b*) and (*c*). This is a consequence of the presence of temperature-dependent dimer diffusion; blocked dimers exist which take some time to become mobile and cannot diffuse freely through the system. Instead of being eliminated before they can make a substantial contribution to the response, some dimers persist and considerably increase the response before they are finally removed. This accounts for the intermediate humps shown for short waiting times in figures 23(*b*) and (*c*); at longer waiting times this effect is imperceptible because the dimers have moved closer to equilibrium. It is also imperceptible at higher temperatures (lower β) because the dimers can move more freely and equilibrate more quickly.

Let us turn now to the overlap function, defined in this case as

$$Q_{t_w}(t) = \frac{\sum_{i=1}^{N} \delta^1_{s_i,0}(t_w + t)\delta^2_{s_i,0}(t_w + t)}{\sum_{i=1}^{N} \delta^1_{s_i,0}(t_w)}. \tag{25}$$

Recalling that in equilibrium one finds $Q(t) = C(2t)$, we can use the equilibrium overlap to test of our proposed form of $C(t)$, as given in equation (22). If this equation holds we expect to find that for short times

$$Q(t) \sim (\alpha e^{-2t/\tau_1} + (1 - \alpha)) \sim \left(\frac{(C(t) + \alpha - 1)^2}{\alpha} + (1 - \alpha) \right) \tag{26}$$

and for long times

$$Q(t) \sim (1 - \alpha) e^{(-2t/\tau_2)^\gamma} \sim \frac{C(t)^{2^\gamma}}{(1 - \alpha)^{2^\gamma}}. \tag{27}$$

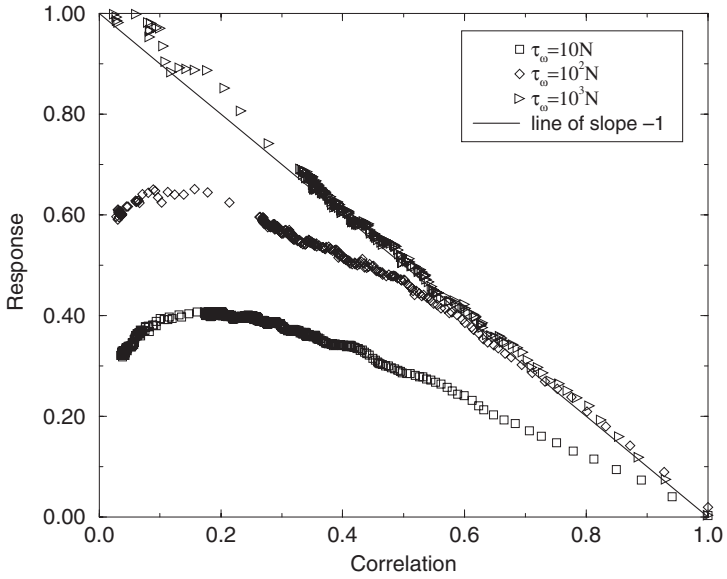

$[\beta = 2.5]$

(*a*)

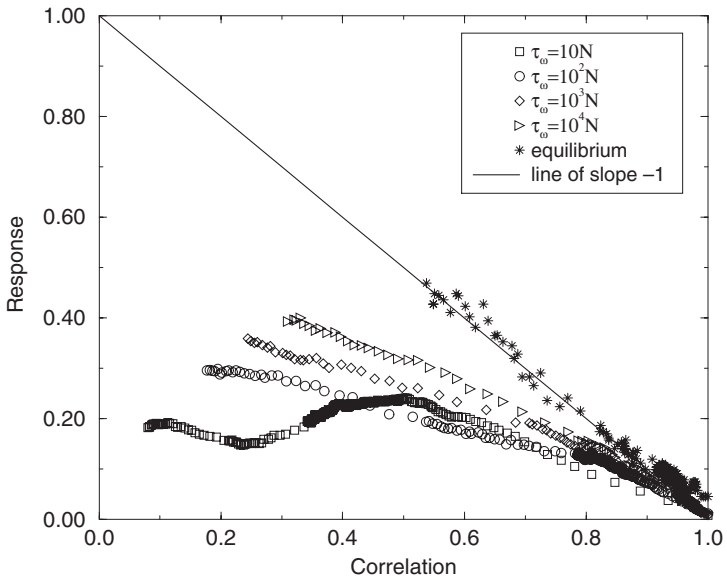

$[\beta = 4.5]$

(*b*)

Figure 23. Parametric plots of the response against the correlation function for different temperatures and waiting times. (*a*) $\beta = 2.5$. (*b*) $\beta = 4.5$. (*c*) (next page) $\beta = 6$.

Figure 24 shows the equilibrium results for $\beta = 2.5$ and 3.5; the superimposed curves are the expected short- and long-time behaviour using the values of α, γ obtained from fitting the correlation functions with equation (22). The theoretical behaviour clearly fits the data very well, lending further support to equation (22) as a description of the behaviour of the

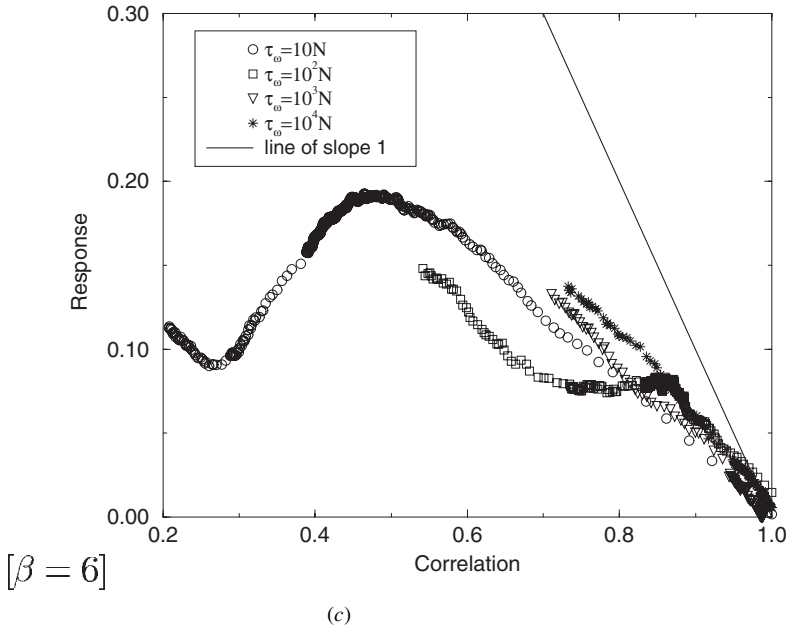

(*c*)

Figure 23. Continued

equilibrium correlation functions. We also see that $Q(t)$ decays to zero, thus placing the $D < 0$ model in the Type II class along with the $D > 0$ model.

5. Concluding remarks

We have studied a simple lattice-based spin model which has a non-interacting Hamiltonian, but constrained dynamics, and find it to exhibit both glassy behaviour and behaviour typical of diffusion-limited reaction models. A single parameter D distinguishes two types of ground state. By choosing $D > 0$, one can study a system with a unique ground state, evolving by way of a number of annihilation–diffusion processes which are either fast temperature-independent or slow temperature-dependent diffusive processes, with the latter slower by a factor exponential in inverse temperature. We can categorize the fast processes as $A + \bar{A} \to \emptyset$, $A + A$ (or $\bar{A} + \bar{A}$) $\to C + \bar{C}$, A (or $\bar{A}$) $+ C$ (or $\bar{C}$) $\to \emptyset + C$ (or $\bar{C}$); and the slow processes as $C + \bar{C} \to A$ (or $\bar{A}$), where A and $\bar{A}$ are dimers and anti-dimers, and C and $\bar{C}$ are isolated defects of opposite sign. The isolated defects move isotropically, but the dimers and anti-dimers move anisotropically, and come in three different 'flavours' according to their orientation. The different flavours can also scatter amongst themselves via the process $A^\alpha + \bar{A}^\alpha \to A^\beta + \bar{A}^\beta$, where α, β label different flavours. Since $A \neq \bar{A}$ and $C \neq \bar{C}$, $A + \bar{A}$ processes are equivalent to the usual $A + B$ processes, and $C + \bar{C}$ are equivalent to $C + D$ processes. In this paper we study the full set of processes simulationally but only provide a simplified adiabatic theoretical fit. For $D < 0$, the ground state is highly degenerate and the system evolves according to the fast annihilation–diffusion processes $A + A \to \emptyset$, $A + A \to C + C$, $A + C \to \emptyset + C$, and the slow diffusive process $C + C \to A$, where A corresponds to a pair of zero-spins and C to an isolated zero-spin. Again there are three different flavours of A corresponding to the three different orientations, and these can scatter through $A^\alpha + A^\alpha \to A^\beta + A^\beta$. In this case the movement of A's are hindered by the background due to the ground state degeneracy, and

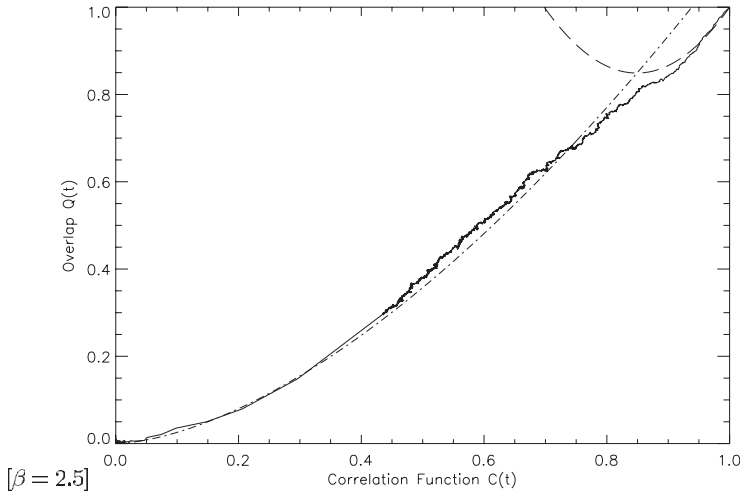

(*a*)

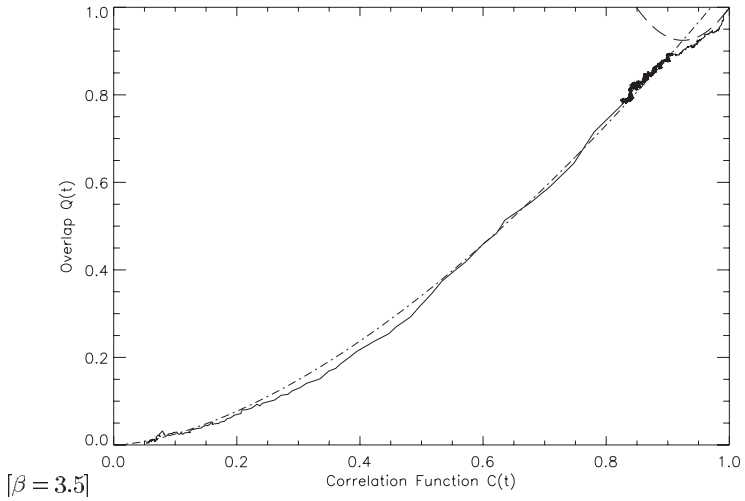

(*b*)

Figure 24. Overlap $Q(t)$ against $C(t)$ in equilibrium. In each case the dashed curve is the expected short-time behaviour and the dot-dashed curve is the expected long-time behaviour, if equation (22) holds. The values of α, γ are those fitted in the previous section. (*a*) $\beta = 2.5$. (*b*) $\beta = 3.5$.

even the fast processes have some temperature dependence. As before we have studied the full dynamics simulationally but only provide a simplified adiabatic analysis. There is clearly scope for providing a full analytic theory.

For both the $D > 0$ and the $D < 0$ case one finds two-step relaxation, on two different timescales which are separable and can be attributed directly to the different processes. We find that the energy in the $D > 0$ case can be fitted with the sum of two terms, each behaving like the asymptotic predictions of an $A + B \to \emptyset$ theory (for the slow processes, $C + \bar{C} \to A$, but the A are eliminated on a timescale which is negligible compared to that of the slow process, so this behaves as $C + \bar{C} \to \emptyset$). In the $D < 0$ case one cannot fit the energy adequately in the approach to the intermediate plateau without including induced dimer absorption ($A + C \to \emptyset + C$)

along with the $A + A \rightarrow \emptyset$ fast diffusive processes. We also find that the slow diffusive process does not behave like a pure $C + C \rightarrow \emptyset$ process; this is in part due to the fact that the dimer diffusion is now temperature dependent. We have studied the correlation functions for D positive and negative; in both cases, a naive theory gives a predicted form for these which fits the data extremely well. Studies of the overlap in equilibrium serve to reinforce these results. An investigation of the response function in both cases yields non-monotonic response curves, and for $D < 0$ the temperature-dependent diffusion leads to more complex results: one finds intermediate humps for very low temperatures and short waiting times, which can be understood within the framework of the processes we have already discussed. Non-monotonicity has also been observed in the response functions of many other models which involve activated processes [3–9, 16]. To distinguish between Type I (coarsening) and Type II (glassy) tendencies we have examined an overlap function measuring the temporal auto-correlation of two independently evolving clones of a configuration. This demonstrates that the present system is of Type II, for D both positive and negative.

In this paper we have employed a hexagonal basis for the cell edges. This is naturally motivated by analogy with a two-dimensional froth. It also corresponds to the case of the simplest non-trivial vertices, which have valence three, and consequently is special in that any cell has two nearest-neighbour cells which are nearest neighbours of one another. Extensions are clearly possible, both to higher valence vertices in two dimensions and to minimal and non-minimal vertices in higher dimensions, but we do not pursue them here. We merely note that systems with valence greater than $(d + 1)$, where d is the dimensionality, are more prone to sticking.

Acknowledgments

The authors would like to thank J Cardy, F Ritort, E Moro and S Krishnamurthy for helpful discussions. LD, DS and JPG would like to thank EPSRC(UK) for financial support: DS and JPG for research grant GR/MO4426, and LD for research studentship 98311155. AB acknowledges the support of Marie Curie Fellowship HPMF-CT-1999-00328. JPG also acknowledges the award of a Violette and Samuel Glasstone Research Fellowship.

References

[1] Davison L and Sherrington D 2000 *J. Phys. A: Math. Gen.* **33** 8615
[2] Aste T and Sherrington D 1999 *J. Phys. A: Math. Gen.* **32** 7049
[3] Fredrikson G H and Andersen H C 1984 *Phys. Rev. Lett.* **53** 1244
[4] Jäckle J and Eisinger S 1991 *Z. Phys.* B **84** 115
[5] Kurchan J, Peliti L and Sellitto M 1997 *Europhys. Lett.* **39** 365
[6] Sollich P and Evans M R 1999 *Phys. Rev. Lett.* **83** 3238
[7] Crisanti A, Ritort F, Rocco A and Sellitto M 2000 *J. Chem. Phys.* **113** 10615
[8] Garrahan J P and Newman M E J 2000 *Phys. Rev.* E **62** 7670
[9] Barrat A, Kurchan J, Loreto V and Sellitto M 2000 *Phys. Rev. Lett.* **85** 5034
[10] Bonilla L L, Padilla F G, Parisi G and Ritort F 1996 *Phys. Rev.* B **54** 4170
Bonilla L L, Padilla F G and Ritort F 1998 *Physica* A **250** 315
[11] Nieuwenhuizen T M 1998 *Phys. Rev. Lett.* **80** 5580
Nieuwenhuizen T M 2000 *Phys. Rev.* E **61** 267
[12] Weaire D and Rivier N 1984 *Contemp. Phys.* **25** 59
[13] Stavans J 1993 *Rep. Prog. Mod. Phys.* **56** 733
[14] Götze W 1999 *J. Phys.: Condens. Matter* **11** A1
[15] Angell C A 1995 *Science* **267** 1924
[16] Nicodemi M 1999 *Phys. Rev. Lett.* **82** 3734
[17] Toussaint D and Wilczek F 1983 *J. Chem. Phys.* **78** 2642

[18] Mattis D C and Glasser M L 1998 *Rev. Mod. Phys.* **70** 979
[19] Hinrichsen H 2000 *Adv. Phys.* **49** 815
[20] Kayser R F and Hubbard J B 1983 *Phys. Rev. Lett.* **51** 79
[21] Grassberger P and Procaccia I 1982 *J. Chem. Phys.* **77** 6281
[22] Stillinger F H and Weber T A 1982 *Phys. Rev.* A **25** 978
[23] Stillinger F H and Weber T A 1984 *Science* **225** 983
[24] Stillinger F H 1995 *Science* **267** 1935
[25] Sastry S, Debenedetti P G and Stillinger F H 1998 *Nature* **393** 554
[26] Sciortino F, Kob W and Tartaglia P 1999 *Phys. Rev. Lett.* **83** 3214
[27] Kob W 1999 *J. Phys. C: Solid State Phys.* **11** R85
[28] Bouchaud J-P, Cugliandolo L, Kurchan J and Mézard M 1998 *Spin Glasses and Random Fields* ed A P Young p 161
[29] Parisi G 1997 *Phys. Rev. Lett.* **79** 3660
[30] Barrat A, Burioni R and Mézard M 1996 *J. Phys. A: Math. Gen.* **29** 1311
[31] Bray A J 1994 *Adv. Phys.* **43** 357